The Effect Of The Crossarms On The Surge Voltage Due To Direct Lightning Strokes On Transmission Line Towers.

TAMBUNAN, Firman. THE EFFECT OF THE CROSSARMS ON THE SURGE VOLTAGE DUE TO DIRECT LIGHTNING STROKES ON TRANSMISSION LINE TOWERS.

Lehigh University, Ph.D., 1959
Engineering, electrical

University Microfilms, Inc., Ann Arbor, Michigan

THE EFFECT OF THE CROSSARMS ON THE SURGE VOLTAGE DUE TO DIRECT LIGHTNING STROKES ON TRANSMISSION LINE TOWERS

by

Firman Tambunan

A DISSERTATION

Presented to the Graduate Faculty

of Lehigh University

in Candidacy for the Degree of

Doctor of Philosophy

Lehigh University

1959

Approved and recommended for acceptance as a dissertation in partial fulfillment of the requirements for the degree of Doctor of Philosophy.

July 20 1959
(Date)

R V Beuley
Professor in Charge

Accepted, July 20, 1959
(Date)

Special committee directing the doctoral work of Mr. Firman Tambunan

R V Beuley Chairman

Vaid V. Latshaw

A R Miller

J B Hartman

ACKNOWLEDGMENTS

The author is indebted to Professor L. V. Bewley, Dean of Engineering of Lehigh University, for his continued encouragement and advice during the preparation of this work.

Thanks are extended to many professors and friends at Lehigh University who encouraged him and helped him during his study at this institution.

Grateful acknowledgment is also made to Mr. Quentin H. Smith Jr., Head of the Steel Tower Design of the Transmission Line Division, PPL, Allentown, for his suggestions and advice in the design of a Double Circuit Suspension Tower.

<u>TABLE OF CONTENTS</u>

INTRODUCTION

Recent experiences of the American Gas and Electric Company (AGE) and the Ohio Electric Corporation (OVEC) indicate that the lightning performance of their 345-kv transmission line systems has been much worse than had been predicted by current theory. According to the prediction their lines should be practically lightning proof, but their experience shows that during the 1955 and 1956 lightning season, they suffered an average of 10.4 flashovers per 100 line-miles per year.(1,2)* The reason for this has not been explained, but investigations were started immediately and have been going on ever since.

A major object of investigation is to determine the effect of the transmission line tower itself on the tower top voltages. How the flashover voltages are produced on the tower during a lightning stroke is not clearly understood. In particular, the surge impedance concept requires a renewed scrutiny.

For some time in over voltage calculations the transmission line tower has been considered as having a single surge impedance. Its calculation is based on the assumption

---

*The numbers between parantheses refer to the bibliography.

that the tower may be represented by a single equivalent cylinder having a uniform charge distribution on its surface. This assumption appears to be justified for towers less than 100' high.

However, recent field tests on transmission line towers higher than 100' show that their surge impedances are tapered. From a test on a 168' tower of a 345-kv line, the surge impedance was found to vary from 135 ohms at the top to 60 ohms at the bottom.[3] From a test[4] on a 108' tower of a 138-kv line, the value of the surge impedance varied from 165 ohms to 108 ohms for the tower isolated and from 165 ohms to 50 ohms with the tower grounded. It is believed that this tapered surge impedance is due to two factors:

1. The vertical position and the height of the tower above the ground.
2. The difference in the dimensions of the various parts of the tower.

The various parts of the tower that may have different surge impedances are:

the bottom part (from the tower footing up to the bottom crossarms),

the upper part (from the bottom crossarms to the tower top but excluding the crossarms) and

the crossarms.

Each of these surge impedances will influence the voltages on the tower.

The effects of the crossarms have not been investigated heretofore. But they may play an important part in the overall lightning performance of the transmission tower. It is therefore the purpose of this dissertation to investigate the effects of the crossarms on the surge voltages due to direct lightning strokes on the tower. The work will be divided into two parts:

1. The calculation of the surge impedances of the various parts of the transmission line tower.
2. The investigation of the effects of the crossarms on the surge voltages due to lightning strokes.

The problem is essentially to determine the surge voltage due to a lightning stroke and to analyze the effects of the crossarms on that voltage. The calculation of the surge voltage will be based upon the standard method, that is by representing the tower by a surge impedance or surge impedances. In the investigation two types of lightning strokes will be considered:

1. An abrupt unit wave.
2. Unit wave with an oblique front.

PART I

Calculation of the surge impedance of the various parts of the transmission line tower.

1.1 Procedure.

A typical 345-kv double-circuit suspension tower, such as used on the AGE and OVEC transmission lines will be investigated.[1,2] A sketch is shown in Fig.1. For the purpose of surge voltage calculation the tower will be divided into three parts:

1. The tower leg (from footing to bottom crossarms).
2. The tower top (from bottom crossarms to tower top excluding crossarms).
3. The crossarms (each assumed to have the same dimensions).

To determine the surge impedance each part will be represented by an equivalent cylinder with the radii calculated according to Fortesque's method.[5] (See Fig.2). Then by Howe's method [6] its capacitance "C" per unit length is determined and finally the surge impedance is found from the following equation:

$$Z = \frac{1}{3 \times 10^8 \, C} \text{ ohms, where C is in f/m.} \qquad (1)$$

1.2 The surge impedance of the tower leg (Z_1).

The bottom part of the tower from the footing to the bottom crossarms, here called the "tower leg", is represented by an equivalent cylinder with a height of 88'(26.8m) and a radius of 7.4'(2.26m). Fig.2 shows a sketch (not to scale) of the tower leg with its equivalent cylinder. The symbols used are the same as in the reference.(5) Referring to the figure the radius is found from the following formula:

$$r = \sqrt[4]{R_m \left(\sqrt{2}\ C^3\right)} = 7.4' \text{ or } 2.26\text{m}. \qquad (2)$$

where R_m (the equivalent radius of each of the four legs composing the "tower leg")

$$= \sqrt[4]{R_m' \ R_m'' \ d^2}$$

$$R_m' = .2235\ (\ a + b\ ) \qquad d^2 = x^2 + y^2$$

$$R_m'' = .2235\ b \qquad x = \frac{b - a}{2}$$

$$a = .75'' \text{ (assumed)} \qquad y = \frac{b}{2}$$

$$b = .80' \text{ (assumed)}$$

$$c = .5\ (\ 33' + 7.25'\ ) = 20'$$

In order to be able to determine the capacitance by Howe's method, it is first assumed that the charge distribution on the surface of the cylinder is uniform, although such an assumption is known to be incorrect, in particular for a vertical cylinder. Fig.3 shows the cylinder with length "h" and height "a" from the ground. The image is shown in broken lines. Assuming a uniform charge distribution on its surface equal to q coulombs per unit length, that is per meter in the MKS system, then the charge density is $q/2\pi r$ coulombs per square meter. The charge on each element of area and its image contribute to the potential at point P on the surface, and the total potential at that point can be determined by adding up all these contributions over the entire surface (and the image) of the cylinder.

To simplify the problem the charged cylinder may be replaced by a line charge situated along the axis of the cylinder and having the same charge per unit length as the surface. Then, referring to Fig.3, the contribution to the potential at point $P(r,z_p)$ on the surface due to the axis charge of an element of length Δz located at point $(0,z)$ with its image at point $(0,-z)$ will be

$$\Delta V = \frac{q\Delta z}{4\pi\varepsilon\sqrt{(z_p-z)^2+r^2}} - \frac{q\Delta z}{4\pi\varepsilon\sqrt{(z_p+z)^2+r^2}} \tag{3}$$

where q is the charge per unit length and ε is the dielectric constant for air having a value of $\frac{1}{36\pi \times 10^9}$.

The total potential at $P(r,z_p)$ due to the assumed charge distribution along the axis is

$$V_p = \frac{q}{4\pi\varepsilon}\int_a^{h+a}\left[\frac{1}{\sqrt{(z_p-z)^2+r^2}} - \frac{1}{\sqrt{(z_p+z)^2+r^2}}\right]dz$$

$$= \frac{q}{4\pi\varepsilon}\left|[\sinh^{-1}\frac{z-z_p}{r} - \sinh^{-1}\frac{z+z_p}{r}]\right|_a^{a+h}$$

$$= \frac{q}{4\pi\varepsilon}[\sinh^{-1}\frac{a+h-z_p}{r} - \sinh^{-1}\frac{a-z_p}{r}$$

$$- \sinh^{-1}\frac{a+h+z_p}{r} + \sinh^{-1}\frac{a+z_p}{r}] \tag{4}$$

The average potential along the cylinder may be found by integrating Eq.4 with respect to z over the length of the cylinder and dividing by h, thus

$$V_{av} = \frac{1}{h}\frac{q}{4\pi\varepsilon}\int_a^{h+a} V_p(z)\,dz \tag{5}$$

The capacitance per unit length is then

$$C = \frac{q}{V_{av}} \tag{6}$$

and Z_1 as found from Eq.1 is

$$Z_1 = \frac{1}{3 \times 10^8 C} = \frac{V_{av}}{3 \times 10^8\, q} =$$

$$= \frac{1}{h}\frac{1}{3 \times 10^8}\frac{1}{4\pi\varepsilon}\int_a^{h+a} V_p(z)\,dz$$

$$= \frac{30}{h}\left|[-(a+h-z)\sinh^{-1}\frac{a+h-z}{r} + \sqrt{(a+h-z)^2 + r^2}\right.$$

$$-(a+h+z)\sinh^{-1}\frac{a+h+z}{r} + \sqrt{(a+h+z)^2 + r^2}$$

$$+(a-z)\sinh^{-1}\frac{a-z}{r} - \sqrt{(a-z)^2 + r^2}$$

$$\left.+(a+z)\sinh^{-1}\frac{a+z}{r} - \sqrt{(a+z)^2 + r^2}\,]\right|_a^{a+h}$$

$$= \frac{30}{h}[\,2r + 2h\sinh^{-1}\frac{h}{r} - 2\sqrt{h^2+r^2}$$

$$-2(a+h)\sinh^{-1}\frac{2(a+h)}{r} + \sqrt{4(a+h)^2+r^2}$$

$$+2(2a+h)\sinh^{-1}\frac{2a+h}{r} - 2\sqrt{(2a+h)^2+r^2}$$

$$-2a\sinh^{-1}\frac{2a}{r} + \sqrt{4a^2+r^2}\,] \qquad (7)$$

Making the substitutions $\ln \frac{h+\sqrt{h^2+r^2}}{r}$ for $\sinh^{-1}\frac{h}{r}$, etc. and simplifying, Eq.7 reduces to Jordan's formula:

$$Z_1 = \frac{30}{h}[\sqrt{4a^2+r^2} - 2(h+a-r) + 2h\ln\frac{h(2a+h)}{r(a+h)}$$

$$+2a\ln\frac{(2a+h)^2}{(h+a)(2a+\sqrt{4a^2+r^2})}\,] \qquad (8)$$

Substituting numerical values and taking a (height above true ground) to be zero, the surge impedance of the tower leg Z_1 is found to be 95 ohms.

1.3 The surge impedance of the tower top (Z_2).

The upper part of the tower from the bottom crossarms to the top, excluding the crossarms is called the "tower top" and is represented by an equivalent cylinder with a height of 18.3m and a radius of 1.1m. The latter is found from Eq.2 by substituting for c = 7.25' or 2.2m and keeping the other values unchanged. The surge impedence is found from Eq. 7 or 8. For a = 26.8m and h = 45.1m, Z_2 = 145 ohms.

1.4 The surge impedance of the crossarms (Z_c).

Each of the three pairs of crossarms will be assumed to have the same surge impedance. Referring to Fig.4, the surge impedance may be found by applying Eqs 3 and 4 to a horizontal cylinder having a height "H" above true ground. After modification Eq.4 becomes

$$V_p = \int_0^L \left(\frac{q\,dx}{4\pi\varepsilon\sqrt{(x-x_p)^2+r^2}} - \frac{q\,dx}{4\pi\varepsilon\sqrt{(x-x_p)^2+4H^2}} \right)$$

where "L" is the length of the crossarm and "r" the radius of the equivalent cylinder. The value of L is the average value of the lengths of the three pairs of crossarms and is taken to be equal to 5.5m. The radius is found to be 0.2m by substituting for a = .75" (assumed), b = .40'(assumed) and c = 7.25' in Eq.2.

As in Eq.5, the average potential V_{av} at the surface of the cylinder is found by integrating V_p with respect to x between the limits 0(zero) and L and dividing by L. Then by substituting V_{av} in Eqs 6 and 1 and integrating, the result is the equation for the surge impedance of the crossarm:

$$Z_c = \frac{60}{L}\left(r-2H-\sqrt{L^2+r^2}+\sqrt{L^2+4H^2}+L\sinh^{-1}\frac{L}{r}-L\sinh^{-1}\frac{L}{2H}\right) \quad (9)$$

Since $2H \gg L$, Eq.9 can be simplified into

$$Z_c = \frac{60}{L}\left(r-\sqrt{L^2+r^2}+L\sinh^{-1}\frac{L}{r}\right)$$

which is independent of the height H above true ground. For $L = 5.5m$ and $r = .2m$, $Z_c = 180$ ohms.

1.5 Other surge impedances involved in the investigation.

The ground wire is a single steel wire with a diameter of 0.576".[3] Taking the average height of the ground wire above true ground to be equal to 140', then the surge impedance of the wire is found from the following equation:

$$Z_g = 60 \ln \frac{2H}{r} \tag{10}$$

For $H = 140'$ and $r = .288"$, $Z_g = 560$ ohms.

The lightning stroke will be assumed to be such as to transmit to the tower a unit voltage wave of infinite length with an abrupt front. Also, the effects of the crossarms on unit voltage waves with oblique fronts of 0.2, 0.4, 0.8 and 1.0 microsecond will be calculated. Throughout the calculations the surge impedance of the lightning stroke is assumed to be equal to 300 ohms.

PART II

Investigation of the effects of the crossarms on the surge voltages due to lightning strokes.

2.1 Procedure.

The problem is to find the surge voltage at a selected point on the tower due to a lightning stroke and to analyze the effects of the crossarms on that voltage.

One point will be at the tip of the upper crossarms, for it is there where the transmission line insulation appears to be most vulnerable to failures due to lightning. In case it is found necessary to omit the upper crossarms from the calculations in some parts of the analysis the voltages will be calculated at the position of the upper crossarms.

The calculation of the surge voltage will be based on the assumption that a tower may be represented by a surge impedance. Use will be made of reflection lattice diagrams, "wave trains" and "retarder operators" as described elsewhere.[8]

If all three pairs of crossarms be considered simultaneously in the calculation of the surge voltage, it is found that because of the relatively large number of junctions and the short distances between them, the work becomes prohibitive. (In the Appendix is shown the approximate result when all the crossarms are taken into consideration.)

Hence the effects of each pair of crossarms on the surge voltage will be studied separately, and based on these findings an approximate method will be used to determine the surge voltage.

2.2 Defining the wave trains and operators.

When a voltage wave $e = f(t)$, coming down the tower, reaches a junction between the tower body and a pair of crossarms, part of the initial wave $e_1 = a_1 f(t)$ is reflected back and another part $e_2 = b_1 f(t)$ is transmitted downward, a_1 and b_1 being the reflection and refraction coefficients at that junction. The transmitted wave proceeds down the tower as well as horizontally to the tips of the crossarms. (See Fig. 5) Assuming no attenuation, the wave $e_2 = b_1 f(t)$ will reach the tips of the crossarms where it will undergo a reflection. Assuming the crossarms to be open at the end, the reflected wave from the tip has the same magnitude as the incident wave. After reaching the tower body, the wave undergoes another reflection, with the result that a wave $e_3 = b_1 A_1 f(t)$ returns to the tip, while waves $e_4 = b_1 B_1 f(t)$ are transmitted both up and down the tower. A_1 and B_1 are the reflection and refraction coefficients at the junction, looking from the crossarms. Note that in Fig. 5 the pair of crossarms is represented by an equivalent single crossarm.

If the wave that is reflected to and fro on the crossarm be traced until it dies out, one will find that as it undergoes reflections at the junction, it generates a series of transmitted waves that go up as well as down the tower. In other words, the first reflected wave $e_1 = a_1 f(t)$ is soon accompanied by a series of waves that follow one another at equal intervals of s microsecond, which is the time required by the waves to travel to and fro on the crossarm. Calling that group of waves a "wave train", this may be expressed mathematically in the following form:

$$
\begin{aligned}
e_{r1} &= a_1 f(t-0s) + b_1 B_1 f(t-s) + b_1 B_1 A_1 f(t-2s) \\
&\quad + b_1 B_1 A_1^2 f(t-3s) + \ldots \quad b_1 B_1 A_1^{m-1} f(t-ms) \\
&= a_1 [1 + \frac{b_1}{a_1} B_1 \sum_1^m A_1^{m-1} \phi(-ms)] f(t) \\
&= a_1 \underline{\alpha}_1 f(t) \qquad (11)
\end{aligned}
$$

In general $e_{rn} = a_n \underline{\alpha}_n f(t)$, where

$$\underline{\alpha}_n = 1 + \frac{b_n}{a_n} B_n \sum_1^m A_n^{m-1} \phi(-ms).$$

$\underline{\alpha}_n$ may be called "reflection operator" while $\phi(-ms)$ is defined as "retarder operator" to be interpreted as follows:

$$\phi(-ms) f(t) = f(t-ms) \qquad (12)$$

Similarly the first transmitted wave down the tower is accompanied by a series of waves to form another wave train, which may be expressed in the following form:

$$e_{t1} = b_1[1 + B_1 \sum_1^m A_1^{m-1} \phi(-ms)]f(t)$$

$$= b_1 \underline{\beta_1} f(t), \tag{13}$$

$\underline{\beta_1}$ being the "refraction operator".

The reflection and refraction operators are called such, because they are always preceded by reflection and refraction coefficients.

To determine the surge voltage at the tip of the crossarm it is necessary to define another refraction operator, which when multiplied by the refraction coefficient b_1 will give the expression for the wave train that proceeds to the tip of the crossarm. Calling that wave train

$$e_{t_1}' = b_1 \underline{\gamma_1} f(t), \tag{14}$$

then $\underline{\gamma_1}$ is the refraction operator and is defined as

$$\underline{\gamma_1} = 1 + \sum_1^m A_1^m \phi(-ms). \tag{15}$$

The application of wave trains and operators is a great help in the construction of the lattice diagrams. As will be shown later on, a group of waves may be represented on the diagrams by a single line and junction points may be replaced by transition points.

To simplify the lattice diagram still further, other wave trains will be introduced, which may be called second order wave trains. They are particularly useful when the lattice diagram has two or more transition points. Referring to Fig.6, let points P_1, P_2, P_3 and P_4 be the positions of the crossarms on the tower and the tower footing respectively. A voltage wave passing through P_1 and going downward is partly transmitted and partly reflected on reaching P_2. The transmitted wave $e_1 = \underline{b}_2 f(t)$ proceeds to P_3 where it undergoes another refraction and reflection. The reflected wave $e_2 = \underline{b}_2\underline{a}_3 f(t)$, which returns to P_2 starts a series of reflections between P_2 and P_3 until it dies out. Each time it reaches a transition point (P_2 or P_3) its magnitude is reduced as part of it is refracted beyond that point.

The transmitted waves through P_3 due to the reflections between P_2 and P_3 will form a wave train which may be expressed in the following equation:

$$\begin{aligned} e_3 &= \underline{b}_2\underline{b}_3 f(t_3 - 0s_3) + \underline{b}_2\underline{b}_3\underline{a}'_2\underline{a}_3 f(t_3 - s_3) + \\ &\quad + \underline{b}_2\underline{b}_3(\underline{a}'_2\underline{a}_3)^2 f(t_3 - 2s_3) + \,..\, \underline{b}_2\underline{b}_3(\underline{a}'_2\underline{a}_3)^m f(t_3 - ms_3) \\ &= \underline{b}_2\underline{b}_3[1 + \sum_1^m(\underline{a}'_2\underline{a}_3)^m \phi(-ms_3)]f(t_3), \end{aligned} \tag{16}$$

in which s_3 is the time required by the wave to travel back and forth between the two points. The reflection and refraction operators at the transition points are defined as follows: $\underline{a}'_2 = a'_2\underline{\alpha}'_2$, $\underline{a}_3 = a_3\underline{\alpha}_3$, $\underline{b}_2 = b_2\underline{\beta}_2$ and $\underline{b}_3 = b_3\underline{\beta}_3$.

Similarly the transmitted waves through P_2 toward the direction of P_1 will form another wave train, which may be expressed in an equation almost similar to Eq.16, thus

$$\begin{aligned} \underline{e}_2 &= \underline{b}_2\underline{a}_3\underline{b}'_2 f(t_2-0s_3) + \underline{b}_2\underline{a}_3\underline{b}'_2\underline{a}'_2\underline{a}_3 f(t_2-s_3) + \dots \\ &\quad + \underline{b}_2\underline{a}_3\underline{b}'_2(\underline{a}'_2\underline{a}_3)^m f(t_2-ms_3) \\ &= \underline{b}_2\underline{a}_3\underline{b}'_2[1 + \overset{m}{\Sigma}(\underline{a}'_2\underline{a}_3)^m\,(-ms_3)]f(t_2). \end{aligned} \tag{17}$$

Calling the terms between the brackets second order operators, because of the presence of the reflection operators in it, it may be noted that they are common to both Eqs 16 and 17. Representing them by a single symbol, say $\underline{C}$, then $\underline{e}_2 = \underline{b}_2\underline{a}_3\underline{b}'_2\underline{C}f(t_2)$ and $\underline{e}_3 = \underline{b}_2\underline{b}_3\underline{C}f(t_3)$. Now they may be represented by single lines on the lattice diagram. (See Fig.6). Note that $\underline{e}_2$ is essentially a train of transmitted waves through P_2 but because of the reflection coefficient a_3 in operator $\underline{a}_3$, it is more convenient to show it as a reflected wave from P_3. However in doing so there is a possibility of making an error in allowing it to undergo a reflection at P_2. To avoid this, the wave train $\underline{e}_2$ is indicated by broken lines between P_3 and P_2.

2.3 Outline of the complete lattice diagram.

The tower under investigation is represented in Fig.7 by the surge impedances of its parts: Z_1=95, Z_2=145, Z_a= Z_b=Z_c=180 ohms, together with Z_g=560 for the ground wire,

$Z_0=300$ (assumed) for the stroke and $R=10$ ohms for the footing resistance.

The distances between the junctions and the lengths of the parts are indicated by the time intervals the wave requires to travel through them. A velocity of propagation of 2.85×10^8 m/s or 940'/μs is assumed, which is somewhat less than the velocity of light.[3,4] Consequently there will be a change in the values of the surge impedances previously calculated. However the change is found so small that it practically does not make any difference in the final result.

In Fig.8 is shown the plan for the complete lattice diagram. P_0, P_1, P_2, P_3 and P_4 are the positions of the tower top, the upper, middle, bottom crossarms and the tower footing respectively. P_1, P_2 and P_3 are reduced from junction points to mere transition points with the understanding that the reflection and refraction coefficients associated with those points will always be accompanied by the reflection and refraction operators as defined in section 2.2 (Eqs 11 and 13). The construction of the complete lattice diagram is further simplified by the application of the second order wave trains.

In Table 1 are compiled the reflection and refraction coefficients and the first and second order operators associated with the transition points. They are

$$a_0' = \frac{Z_g Z_0 - Z_2 Z_g - 2Z_2 Z_0}{Z_0 Z_g + Z_g Z_2 + 2Z_2 Z_0} \qquad b_0 = \frac{2Z_g Z_2}{Z_0 Z_g + Z_g Z_2 + 2Z_2 Z_0}$$

$$a_1 = a_1' = -\frac{Z_2}{Z_a + Z_2} \qquad b_0' = \frac{2Z_g Z_0}{Z_0 Z_g + Z_g Z_2 + 2Z_2 Z_0}$$

$$a_2 = a_2' = -\frac{Z_2}{Z_b + Z_2} \qquad b_1 = b_1' = \frac{Z_a}{Z_a + Z_2}$$

$$a_3 = \frac{Z_c Z_1 - Z_c Z_2 - 2Z_1 Z_2}{Z_c Z_1 + Z_c Z_2 + 2Z_1 Z_2} \qquad b_2 = b_2' = \frac{Z_b}{Z_b + Z_2}$$

$$a_3' = \frac{Z_c Z_2 - Z_c Z_1 - 2Z_1 Z_2}{Z_c Z_1 + Z_c Z_2 + 2Z_1 Z_2} \qquad b_3 = \frac{2Z_c Z_1}{Z_c Z_1 + Z_c Z_2 + 2Z_1 Z_2}$$

$$a_4 = \frac{R - Z_1}{R + Z_1} \qquad b_3' = \frac{2Z_c Z_2}{Z_c Z_1 + Z_c Z_2 + 2Z_1 Z_2}$$

$$A_1 = A_2 = \frac{Z_2 - Z_a}{Z_2 + Z_a} \quad \text{since } Z_a = Z_b \qquad B_1 = B_2 = \frac{2Z_2}{Z_2 + Z_a}$$

$$A_3 = \frac{2Z_1 Z_2 - Z_c Z_1 - Z_c Z_2}{Z_c Z_1 + Z_c Z_2 + 2Z_1 Z_2} \qquad B_3 = \frac{4Z_1 Z_2}{Z_c Z_1 + Z_c Z_2 + 2Z_1 Z_2}$$

$$\underline{\alpha}_n = 1 + \frac{b_n}{a_n} B_n \sum_1^m A_n^{m-1} \phi(-ms)$$

$$\underline{\alpha}_n' = 1 + \frac{b_n'}{a_n'} B_n \sum_1^m A_n^{m-1} \phi(-ms)$$

$$\underline{\beta}_n = \underline{\beta}_n' = 1 + B_n \sum_1^m A_n^{m-1} \phi(-ms)$$

$$\underline{A} = 1 + \sum_1^m (a_1 \underline{\alpha}_1 a_0')^m \phi(-ms_1) \qquad \underline{B} = 1 + \sum_1^m (a_2 \underline{\alpha}_2 a_1' \underline{\alpha}_1')^m \phi(-ms_2)$$

$$\underline{C} = 1 + \sum_1^m (a_2 \underline{\alpha}_2 a_3' \underline{\alpha}_3')^m \phi(-ms_2) \qquad \underline{D} = 1 + \sum_1^m (a_4 a_3' \underline{\alpha}_3')^m \phi(-ms\ )$$

Note that the value of m is different in each operator. Whenever two or more operators appear in the same equation the m is replaced by another symbol. For example

$$\underline{\alpha}_1 \underline{\alpha}_2 = [1 + \frac{b_1}{a_1} B_1 \sum_1^k A_1^{k-1} \phi(-ks)][1 + \frac{b_2}{a_2} B_2 \sum_1^{\ell} A_2^{\ell-1} \phi(-\ell s)].$$

By tracing all the wave trains on the complete lattice diagram, the number of the waves that arrive at P_1 within a certain time interval can be computed. To determine the surge voltage at the tip of the upper crossarms each wave should be multiplied by $\underline{E} = 2\gamma_1$, in which the 2 accounts for the fact that the tip is an open end.

Table 2 contains the important wave trains that arrive at the tip within the first 0.6 microsecond after the incidence of the initial wave.

2.4 The effect of the bottom crossarms on the surge voltage due to an abrupt unit wave coming down from the tower top.

To simplify the problem the upper and middle crossarms will be ignored. The surge voltage will be calculated at the position of the upper crossarms rather than at the tip. The omission of the two pairs of crossarms from the calculation reduces the number of wave trains considerably. Fig.9 shows the complete lattice diagram for the simplified case. The wave trains that arrive at P_1 between 0 and 0.6 microsecond are computed and compiled in Table 3. Substituting numerical values for $a_0'=0$, $a_3=-.52$, $b_3=+.48$, $b_3'=+.74$, $a_3'=-.26$, $A_3=-.22$, $B_3=+.78$ and $a_4=-.81$, there results Table 4. Note that in both tables the initial wave is $e = 1(t)$, of which the actual value is $b_0(=.48)$ times the magnitude of the lightning stroke. Based on Table 4, the surge voltage at P_1 is computed and plotted in Fig.10 (shown in full lines).

If the surge impedance Z_1 be made equal to Z_2 and the value of the footing resistance be raised to 15 ohms in order to keep the value of a_4 constant and equal to -.81, then $a_3=a_3'=-.45$, $b_3=b_3'=+.55$, $A_3=-.11$, $B_3=+.89$ and Table 3 will change into Table 5. In Fig.11 is shown the plot of the surge voltage based on Table 5.

On studying Figs 10 and 11 the following observations are made.

1. At t=.096 microsecond, the surge voltage experiences a dip. But it soon recovers to a value equal to $\frac{2Z_1}{Z_1+Z_0'}$ 1(t), in which Z_0' is the equivalent surge impedance of a parallel combination of lightning stroke and ground wire and is equal to 145 ohms. The recovery is accompanied by damped oscillations and is practically completed at t=.2 microsecond.
2. At t=.284 microsecond the surge voltage decreases sharply but it can be seen that though accompanied by damped oscillations, it follows an exponential curve.
3. At t=.472 microsecond there is another dip, which is smaller in magnitude than the first one. It also recovers very soon to a value equal to $\frac{2R}{R+Z_0'}$ 1(t), which is also the final value of the surge voltage. As in the former case this process is accompanied by damped oscillations.

From Tables 3, 4 and 5 it is seen that the first dip is caused by wave train #2, that is by $e = \underline{a}_3 1(t-.096)$. The decrease after 0.284 microsecond is caused by the first part of wave train #6, namely by $e = \underline{b}_3 a_4 \underline{b}_3' 1(t-.284)$ and the second dip is caused by the second part of wave train #6, that is by $e = \underline{b}_3 a_4^2 \underline{b}_3' \underline{a}_3' 1(t-.472)$. Since the reflection and refraction coefficients are constants, the factors responsible for the recovery of the dips (obs. 1 and 3) and the gradual ending of the decrease (obs. 2) must be the operators.

In Figs 12 and 13 are plotted $\underline{\alpha}_3 1(t)$ and $\underline{\beta}_3 1(t)$ with respect to time. The data used are from Table 5, which give the operators the following values:

$$\underline{\alpha}_3 = 1 - 1.09\phi(-.036) + .12\phi(-.072) - .013\phi(-.108)$$

$$\underline{\beta}_3 = 1 + .89\phi(-.036) - .098\phi(-.072) + .011\phi(-.108)$$

By inspection of the figures it is found that $\underline{\alpha}_3 1(t)$ and $\underline{\beta}_3 1(t)$ may be expressed approximately in the following forms:

$$\underline{\alpha}_3 1(t) = c_1 \varepsilon^{-\alpha t} + c_2 \varepsilon^{-\beta t} \sin\omega_1 t + \ldots\ldots$$

$$= 2.19\varepsilon^{-\alpha t} + c_2 \varepsilon^{-\beta t} \sin\omega_1 t + \ldots\ldots \tag{18}$$

$$\underline{\beta}_3 1(t) = 1.81(1-\varepsilon^{-\alpha t}) + c_3 \varepsilon^{-\gamma t} \sin\omega_2 t + \ldots\ldots \tag{19}$$

The constant coefficient c_1 in Eq.18 is found as follows. Knowing that $b_3\underline{\beta}_3 - a_3\underline{\alpha}_3$ must always be equal to unity, then by putting $t=0$, $\underline{\beta}_3 1(t)$ becomes zero and hence $-a_3\underline{\alpha}_3$ must be equal to unity at that instant. For $a_3=-.45$, $c_1=2.19$. The constant coefficient of the first term in Eq.19 is found either by putting $t=\infty$ or by inspection of Fig.13.

The first exponential terms in both equations are assumed to have the same time constant. This is based on the following consideration. If the oscillatory terms in both equations be neglected in order to simplify further the expressions, then $a_3\underline{\alpha}_3 1(t) = -\varepsilon^{-\alpha t}$, $b_3\underline{\beta}_3 1(t) = 1-\varepsilon^{-\alpha t}$ and $b_3\underline{\beta}_3 - a_3\underline{\alpha}_3$ will still be equal to unity. This leads to the conclusion that when the incident wave is a unit wave, the reflected and transmitted wave from and through a junction point formed by the tower body and a pair of crossarms are by approximation equal to $e_r = -\varepsilon^{-\alpha t}$ and $e_t = 1-\varepsilon^{-\alpha t}$ respectively.

It is known that when two surge impedances in series be shunted at the transition point by a capacitance to ground, forming a junction point, the reflection and refraction at that point to a unit incident wave show similar phenomena. Hence as an approximation the effect of the crossarms may be assumed to be similar to that of an equivalent lumped capacitance, shunted at the position of the crossarms to ground.

2.5 Representing the bottom crossarms by an equivalent lumped capacitance.

From Eq.1 the value of the equivalent capacitance per unit length may be found. The total capacitance C_c that represents the pair of crossarms is 5.5 times that value and for $Z_c = 180$ ohms, C_c is found to be equal to 2.03×10^{-10} farads. Referring to Fig.14, the reflection and refraction operators at the junction point P_3, using Heaviside's operators, are:

$$\underline{b}_3 = \frac{\dfrac{2}{C_c Z_2}}{p+\dfrac{Z_1+Z_2}{Z_1 Z_2 C_c}} = \frac{\alpha}{p+\gamma} \qquad \underline{a}_3 = \underline{b}_3 - 1 = \frac{\alpha-\gamma-p}{p+\gamma}$$

$$\underline{b}_3' = \frac{\dfrac{2}{C_c Z_1}}{p+\dfrac{Z_1+Z_2}{Z_1 Z_2 C_c}} = \frac{\beta}{p+\gamma} \qquad \underline{a}_3' = \underline{b}_3' - 1 = \frac{\beta-\gamma-p}{p+\gamma}$$

where $\alpha = 68 \times 10^6$, $\beta = 104 \times 10^6$ and $\gamma = 86 \times 10^6$. Substituting these values in Table 3, solving and putting $a_0' = 0$ and $a_4 = -.81$, there results Table 6. (The solutions are found from Heaviside's Operational Calculus).[9] Based on Table 6, the surge voltage is plotted and is shown in broken lines in Fig.10.

If the value of Z_1 be made equal to Z_2 and the value of R be raised to 15 ohms to keep a_4 constant and equal to $-.81$, then $\underline{a}_3 = \underline{a}_3' = -\frac{p}{p+\alpha}$ and $\underline{b}_3 = \underline{b}_3' = +\frac{\alpha}{p+\alpha}$, in which $\alpha = 68 \times 10^6$. Solving the operational equations and plotting the curve, the result is shown in broken lines in Fig.11.

It can be shown that with regard to the surge voltage at P_1 or at the tip of the upper crossarms, the middle crossarms will have the same effect as the bottom crossarms. The only difference between the two is the time at which their effect is felt at P_1.

2.6 The effect of the upper crossarms on the surge voltage at its tip due to an abrupt unit wave coming down from the tower top.

To simplify the analysis the middle and the bottom crossarms are ignored. Further it is assumed that $Z_1 = Z_2 =$ 145 ohms and R is raised from 10 to 15 ohms to keep a_4 equal to -.81. Under this condition the complete lattice diagram is very simple as shown in Fig.15. Remembering that $a'_0 =$ 0, the voltage waves that arrive at P_1 between 0 and 0.6 microsecond can be easily read off the lattice diagram. They are:

1. $\underline{b}_1 1(t)$
2. $\underline{b}_1 a_4 \underline{b}'_1 1(t-.284)$
3. $\underline{b}_1 a_4 \underline{a}'_1 \underline{b}'_1 1(t-.568)$

As has been pointed out earlier these do not give automatically the sum of the waves that reach the tip of the upper crossarms within that time interval. However it may be found from the above expressions if they are slightly modified. Replacing $\underline{b}_1 (= b_1 \underline{\beta}_1)$ by $b_1 \underline{E}$, where $\underline{E} = 2\underline{\gamma}$, and $\underline{b}'_1 (= b'_1 \underline{\beta}'_1)$ by $b'_1 \underline{E}$ in the above expressions will give the equations for the wave trains that arrive and reflected at the tip of the upper crossarms. This is done in Table 7. Fig.16 shows the plot in full lines of the surge voltage based on Table 7.

A study of Fig.16 leads to the following observations:

1. The surge voltage starts with a hump making its magnitude temporarily larger than unity. However it

quickly drops to a value of $\frac{2Z_1}{Z_1+Z_0'}$ 1(t), which lasts until t=.284 microsecond. Thus between 0 and 0.284 microsecond the surge voltage shows a dissimilarity with that of the former case, for there it experienced a dip at t=.096 microsecond.

2. At t=.284 microsecond the surge voltage decreases sharply at first, then levels off exponentially until 0.568 microsecond, when it experiences a momentary dip which quickly recovers to a value of $\frac{2R}{R+Z_0'}$ 1(t), thus showing a similarity with the former case. This is particularly obvious in Figs 11 and 16.

The hump as can be learned from Table 7 is caused by the first wave train in the series, namely by $e=b_1\underline{E}1(t)$. If the latter be further analyzed, it can be shown (Fig.17) that it consists of a unit function plus a series of damped oscillations or

$$b_1\underline{E}1(t) = 1(t) + C_1\varepsilon^{-\alpha t}\sin\omega_1 t + \ldots\ldots \qquad (20)$$

$\cong$ 1(t) if the oscillatory terms be neglected.

Putting $b_1\underline{E}1(t)=1(t)$ in the wave equations of Table 7 will reduce them to expressions which contain no other operators than $\underline{a}_1$ and $\underline{b}_1$ (incl. $\underline{a}_1'$ and $\underline{b}_1'$).

It has been shown in section 2.4 that $\underline{a}_1 1(t)$ and $\underline{b}_1 1(t)$ are approximately equal to $-\varepsilon^{-\alpha t}$ and $1-\varepsilon^{-\alpha t}$ respectively. Therefore similar to the bottom crossarms the upper crossarms may also be represented by an equivalent lumped capacitance.

2.7 Representing the upper crossarms by an equivalent lumped capacitance.

The equivalent lumped capacitance representing the upper crossarms is the same as found in section 2.5, that is $C_a = C_c = 2.03 \times 10^{-10}$ farads. Then, referring back to Fig. 14, for $Z_1 = Z_2 = 145$ ohms, $\underline{a}_1 = \underline{a}_1' = -\frac{p}{p+\alpha}$ and $\underline{b}_1 = \underline{b}_1' = +\frac{\alpha}{p+\alpha}$, in which $\alpha = 68 \times 10^6$.

From the lattice diagram in Fig. 15 the waves that arrive at P_1 between 0 and 0.600 microsecond can be computed. As has been pointed out in section 2.6, in order to find the surge voltage at the tip of the upper crossarms, the last $\underline{b}_1$ or $\underline{b}_1'$ in each equation should be replaced by $b_1\underline{E}$ or $b_1'\underline{E}$ and as an approximation the value of the latter should be made equal to unity. This is done in Table 8. This is essentially Table 7 using Heaviside's operators. The resultant surge voltage is plotted in broken lines in Fig. 16.

2.8 Considering the crossarms as integral parts of the tower top.

Figs 10, 11 and 16 demonstrate, that the crossarms may be represented by lumped capacitances. As a further approximation, the capacitances may be assumed to be evenly distributed on the tower top. This will increase the latter's capacitance per unit length and lower the value of its surge impedance. The equivalent capacitance per unit length of the tower top will then be equal to 5.63×10^{-10} f/m and correspondingly the surge impedance, as found from Eq. 1, is $Z_s =$ 59 ohms.

The determination of the surge voltage is now simple. Using Fig. 9 as the complete lattice diagram, the wave trains that arrive at P_1 between 0 and 0.600 microsecond are given in Table 3. Because of the change in the value of Z_s the value of the coefficients will also change. Under the new condition they are: $b_o = +.28$, $a_o' = +.42$, $a_3 = +.23$, $b_3 = 1.23$, $a_3' = -.23$, $b_3' = +.77$ and $a_4 = -.81$. Substituting these values in the equations of Table 3 gives Table 9, from which curve #1 in Fig. 18 is prepared. Note that in Table 9 the value of the unit voltage, due to the change of the value of b_o from 0.48 to 0.28, has decreased to 58% of the one previously defined.

Curve #2 in Fig. 18 is prepared from Table 10, in which the coefficients and operators are calculated in the Appendix. The curve is shown first in full lines until 0.1 microsecond, but because of the great number of oscillations of which the curve is made up, the last part of it is drawn in broken lines, indicating only the approximate axis of oscillations. As can be seen from the figure, the two graphs, except at the time between 0 and 0.1 microsecond, show a similarity. This leads to the conclusion that as an approximate method for determining the surge voltage at the tip of the crossarms or at any other point on the tower as the case may be, the crossarms may be considered as integral parts of the tower top.

2.9 The effect of the crossarms on the surge voltage due to a unit wave with an oblique front.

To simplify the problem, let the tower be assumed to have only the bottom crossarms. Representing the latter by a surge impedance, the surge voltage at P_1 due to a unit wave with an oblique front is calculated. The result is plotted in Fig. 19. To avoid repetition of what has been done before, the effect will be analyzed by way of comparison, namely by comparing the result with another surge voltage due to the same type of wave, but not effected by any crossarm. This is done in Fig. 19. Referring to the figure, the solid lines represent the surge voltage calculated for the tower with no crossarms, while the broken lines are for the tower with crossarms. Graphs #2 to #5 show the voltages due to a unit wave with a front of 0.2, 0.4, 0.8 and 1.0 microsecond respectively. The data for the graphs are based on Table 4.

As can be seen from Fig. 19, the crossarms have only effect on surge voltages due to waves with very steep fronts, while voltages due to waves with fronts longer than 0.2 microsecond are practically uneffected by them. This phenomenon also explains why a crossarm may be represented by an equivalent lumped capacitance. The longer the wave fronts, the smaller is the reflected wave from the junction point. Analytically it can be shown as follows. Referring back to Fig. 14, it is found that when the two surge impedances in series are of the same magnitude, the reflection and refraction operator at the junction are $\underline{a} = -\frac{p}{p+\alpha}$ and $\underline{b} = +\frac{\alpha}{p+\alpha}$. Let the incident wave be a unit wave with a front of Θ_n microsecond, given by the equation:

$$e = \frac{1}{\Theta_n}[t1(t) - (t-\Theta_n)1(t-\Theta_n)], \tag{21}$$

then the reflected and transmitted wave are

$$\begin{aligned}
e_r &= -\frac{p}{p+\alpha}\frac{1}{\Theta_n}[t1(t) - (t-\Theta_n)1(t-\Theta_n)] \\
&= -\frac{1}{\alpha\Theta_n}(1-\varepsilon^{-\alpha t})1(t) + \frac{1}{\alpha\Theta_n}[1-\varepsilon^{-\alpha(t-\Theta_n)}]1(t-\Theta_n) \\
e_t &= +\frac{\alpha}{p+\alpha}\frac{1}{\Theta_n}[t1(t) - (t-\Theta_n)1(t-\Theta_n)] \\
&= (\frac{t}{\Theta_n}-\frac{1}{\alpha\Theta_n}+\frac{1}{\alpha\Theta_n}\varepsilon^{-\alpha t})1(t) - [\frac{(t-\Theta_n)}{\Theta_n}-\frac{1}{\alpha\Theta_n}+\frac{1}{\alpha\Theta_n}\varepsilon^{-\alpha(t-\Theta_n)}] \\
&\quad \times 1(t-\Theta_n).
\end{aligned} \tag{22}$$

Substituting numerical values for Θ_n will show that the larger its value, meaning the longer the wave fronts, the smaller is the magnitude of e_r, while that of e_t becomes larger and approaching unity. In other words, the longer the wave fronts the lesser is the effect of the crossarm on the surge voltage.

CONCLUSION

The effects of the crossarms may be summed up as follows:

1. On the surge voltage due to an abrupt unit wave, given by the equation: $e = 1(t)$, the effect is primarily the same as that of an equivalent lumped capacitance, shunted between the tower and the ground at the position of the crossarms. A secondary effect is the generation of damped oscillations.
2. On the surge voltage due to a unit wave with an oblique front given by the equation: $e = \frac{1}{\theta_n}[t1(t) - (t-\theta_n)1(t-\theta_n)]$, the effect is also the same as that of an equivalent capacitance representing the crossarms. The intensity of the effect is inversely proportional to the length of the wave front. In the case of the transmission line tower that has been investigated, the effect is practically non-existent when the wave front is longer than 0.4 microsecond.

This leads to the conclusion that for the purpose of surge voltage calculations the crossarms may be represented by equivalent lumped capacitances. As a further approximation they may be considered as integral parts of the tower top.

APPENDIX

A. Considering all three pairs of crossarms simultaneously in the calculation of the surge voltage.

Table 2 contains the important wave trains that arrive and are refracted at the tip of the upper crossarms between 0 and 0.6 microsecond, with all the crossarms being included in the calculations. They are obtained through a rigorous method, namely by computing the reflected and transmitted waves in a complete lattice diagram. The latter is not shown here. Judging from the number of wave trains and the complexity of multiplications in them, if numerical values be substituted without simplification, the calculation is prohibitive. Hence a surge impedance of $Z_0 = 300$ ohms is assumed for the lightning stroke to make the reflection coefficient at P_0 looking from the bottom side equal to $a_0' = 0$. This reduces the number of wave trains considerably and for $a_1 = a_2 = a_1' = a_2' = -.45$, $b_1 = b_2 = b_1' = b_2' = +.55$, $a_3 = -.52$, $b_3 = .48$, $a_3' = -.26$, $b_3' = +.74$, $A_1 = -.11$, $B_1 = +.89$, $A_2 = -.22$, $B_2 = +.78$ and $a_4 = -.81$, Table 2 becomes Table 10, in which

$$\underline{B} = 1 + \sum_1^m (.202\underline{a}_2\underline{a}_1')^m \phi(-.050m)$$

$$\underline{C} = 1 + \sum_1^m (.234\underline{a}_3\underline{a}_2')^m \phi(-.046m)$$

$$\underline{D} = 1 + \sum_1^m (.21\underline{a}_3')^m \phi(-.188m)$$

$$\underline{E} = 2 + 2\sum_1^m (-.11)^m \phi(-.036m)$$

$$\underline{a}_1 = \underline{a}_2 = \underline{a}_1' = \underline{a}_2' = 1 - 1.09\sum_1^m (-.11)^{m-1} \phi(-.036m)$$

$$\underline{\beta}_1=\underline{\beta}_2=\underline{\beta}_1'=\underline{\beta}_2' = 1 + .89\sum_1^m(-.11)^{m-1}\phi(-.036m)$$

$$\underline{\alpha}_3 = 1 - .78\sum_1^m(-.22)^{m-1}\phi(-.036m)$$

$$\underline{\alpha}_3' = 1 - 2.22\sum_1^m(-.22)^{m-1}\phi(-.036m)$$

$$\underline{\beta}_3=\underline{\beta}_3' = 1 + .78\sum_1^m(-.22)^{m-1}\phi(-.036m)$$

The result of the calculations is plotted in Fig. 18.

B. Example of solutions given in Tables 6 and 8 and in Eq. 22.

$$\frac{p}{p+\alpha}\,1(t) = \varepsilon^{-\alpha t}1(t),$$

$$\frac{p}{p+\alpha}\,1(t-.096) = \varepsilon^{-\alpha(t-.096)}1(t-.096),$$

$$\frac{\alpha}{p+\alpha}\,1(t) = (1-\varepsilon^{-\alpha t})1(t),$$

$$\frac{p}{p+\alpha}\,(1-\varepsilon^{-\alpha t})1(t) = \alpha t\varepsilon^{-\alpha t}1(t) = \frac{\alpha}{p+\alpha}\,\varepsilon^{-\alpha t}1(t),$$

$$\frac{p}{p+\alpha}\,t\varepsilon^{-\alpha t}1(t) = (1-\frac{\alpha t}{2})t\varepsilon^{-\alpha t}1(t),$$

$$\frac{\alpha}{p+\alpha}\,t1(t) = (t-\frac{1}{\alpha}+\frac{1}{\alpha}\varepsilon^{-\alpha t})1(t),$$

$$\frac{p}{p+\alpha}\,t1(t) = (\frac{1}{\alpha}-\frac{1}{\alpha}\varepsilon^{-\alpha t})1(t),$$

$$\frac{p}{p+\alpha}\,(t-\theta_n)1(t-\theta_n) = [\frac{1}{\alpha}-\frac{1}{\alpha}\varepsilon^{-\alpha(t-\theta_n)}]1(t-\theta_n),$$

where $1(t)$ or $1(t-\theta_n)$ is a unit function, acting only when t or $t-\theta_n$ is positive.

Table 1. Reflection and refraction coefficients, first and second order operators associated with P_0, P_1, P_2, P_3 and P_4.

	Coefficients		Operators	
	Downward and upward	Horizontal	First order	Second order
P_0	b_0' a_0' b_0			$\underline{A}$
P_1	a_1 b_1' a_1' b_1	B_1 A_1	$\underline{\alpha_1}$ $\underline{\beta_1'}$ $\underline{\alpha_1'}$ $\underline{\beta_1}$	$\underline{B}$ $\underline{A}$
P_2	a_2 b_2' a_2' b_2	B_2 A_2	$\underline{\alpha_2}$ $\underline{\beta_2'}$ $\underline{\alpha_2'}$ $\underline{\beta_2}$	$\underline{C}$ $\underline{B}$
P_3	a_3 b_3' a_3' b_3	B_3 A_3	$\underline{\alpha_3}$ $\underline{\beta_3'}$ $\underline{\alpha_3'}$ $\underline{\beta_3}$	$\underline{D}$ $\underline{C}$
P_4	a_4			$\underline{D}$

Table 2. The important wave trains that arrive at the tip of the upper crossarms between 0 and 0.6 microsecond with all the crossarms being considered.

1	$b_1\underline{AE}f(t)$
2	$b_1\underline{a_2}\,\underline{b'_1}\,\underline{ABE}f(t-.050)$
3	$b_1\underline{b_1}\,\underline{a_2}\,\underline{b'_1}a'_0\underline{A}^2\underline{BE}f(t-.082)$
4	$\underline{b_1}\,\underline{b_2}\,\underline{a_3}\,\underline{b'_2}b'_1\underline{AB^2}\,\underline{CE}f(t-.096)$
5	$b_1\underline{b_1}\,\underline{b_2}\,\underline{a_3}\,\underline{b'_2}\,\underline{b'_1}a'_0\underline{A}^2\underline{B}^2\underline{CE}f(t-.128)$
6	$\underline{b_1^2}\,\underline{a_2^2}\,\underline{b'_1}b'_1a'_0\underline{A}^2\underline{B}^2\underline{E}f(t-.132)$
7	$b_1\underline{b_1^2}\,\underline{a_2^2}\,\underline{b'^2_1}a'^2_0\underline{A}^2\underline{B}^2\underline{E}f(t-.164)$
8	$2\underline{b_1^2}\,\underline{b_2}\,\underline{a_3}\,\underline{b'_2}\,\underline{b'_1}b'_1\underline{a_2}a'_0\underline{A}^2\underline{B}^3\underline{CE}f(t-.178)$
9	$\underline{b_1}\,\underline{b_2^2}\,\underline{a_3^2}\,\underline{b'^2_2}\,\underline{a'_1}b'_1\underline{AB^3}\,\underline{C}^2\underline{E}f(t-.192)$
10	$2b_1\underline{b_1^2}\,\underline{a_2}\,\underline{b'^2_1}a'^2_0\underline{b_2}\,\underline{a_3}\,\underline{b'_2}\underline{A}^3\underline{B}^3\underline{CE}f(t-.210)$
11	$b_1\underline{b_1^2}\,\underline{a_2^3}\,\underline{b'^3_1}a'^2_0\underline{A}^3\underline{B}^3\underline{E}f(t-.214)$
12a	$b_1\underline{b_1}\,\underline{b_2^2}\,\underline{a_3^2}\,\underline{b'^2_2}\,\underline{b'^2_1}a'_0\underline{A}^2\underline{B}^4\underline{C}^2\underline{E}f(t-.224)$
12b	$b_1\underline{b_1}\,\underline{b_2^2}\,\underline{a_3^2}\,\underline{b'^2_2}\,\underline{b'_1}\,\underline{a'_1}a'_0\underline{A}^2\underline{B}^3\underline{C}^2\underline{E}f(t-.274)$
13	$b_1\underline{b_1^2}\,\underline{b_2^2}\,\underline{a_3^2}\,\underline{b'^2_2}\,\underline{b'^2_1}a'^2_0\underline{A}^3\underline{B}^4\underline{C}^2\underline{E}f(t-.256)$
14	$\underline{b_1}\,\underline{b_2}\,\underline{b_3}a_4\underline{b'_3}\,\underline{b'_2}b'_1\underline{AB^2}\,\underline{C}^2\underline{DE}f(t-.284)$
15	$b_1\underline{b_1^2}\,\underline{b_2^2}\,\underline{a_3^2}\,\underline{b'^2_2}\,\underline{b'^3_1}\,\underline{a_2}a'^2_0\underline{A}^3\underline{B}^5\underline{C}^2\underline{E}f(t-.306)$
16	$b_1\underline{b_1}\,\underline{b_2}\,\underline{b_3}a_4\underline{b'_3}\,\underline{b'_2}\,\underline{b'_1}a'_0\underline{A}^2\underline{B}^2\underline{C}^2\underline{DE}f(t-.316)$
17	$\underline{b_1^2}\,\underline{b_2^3}\,\underline{a_3^3}\,\underline{b'^3_2}\,\underline{b'^2_1}b'_1a'_0\underline{A}^2\underline{B}^5\underline{C}^3\underline{E}f(t-.320)$
18	$b_1\underline{b_1^2}\,\underline{b_2^3}\,\underline{a_3^3}\,\underline{b'^3_2}\,\underline{b'^3_1}a'^2_0\underline{A}^3\underline{B}^6\underline{C}^3\underline{E}f(t-.352)$
19	$2\underline{b_1^2}\,\underline{b_2}\,\underline{b_3}a_4\underline{b'_3}\,\underline{b'_2}\,\underline{b'_1}b'_1\underline{a_2}a'_0\underline{A}^2\underline{B}^3\underline{C}^2\underline{DE}f(t-.366)$
20	$\underline{b_1}\,\underline{b_2^2}\,\underline{a_3}\,\underline{b'^2_2}\,\underline{b_3}a_4\underline{b'_3}\,\underline{a'_1}b'_1\underline{AB^3}\,\underline{C}^3\underline{DE}f(t-.380)$

Table 2 (ctd).

21	$b_1\underline{b}_1^3\underline{b}_2^3\underline{a}_3^2\underline{b}_2'^3\underline{b}_1'^3\underline{a}_3 a_0'^3\underline{A}^4\underline{B}^6\underline{C}^3\underline{E}f(t-.384)$
22	$2b_1\underline{b}_1^2\underline{b}_2\underline{b}_2 a_4\underline{b}_3'\underline{b}_2'\underline{b}_1'^2\underline{a}_2 a_0'^2\underline{A}^3\underline{B}^2\underline{C}^2\underline{DE}f(t-.398)$
23a	$2\underline{b}_1^2\underline{b}_2^2\underline{a}_2\underline{b}_2'^2 b_1'\underline{b}_1' a_0'\underline{b}_3 a_4\underline{b}_3'\underline{A}^2\underline{B}^4\underline{C}^3\underline{DE}f(t-.412)$
23b	$b_1\underline{b}_1\underline{b}_2^2\underline{a}_3\underline{b}_2'^2\underline{a}_1'\underline{b}_3 a_4\underline{b}_2'\underline{b}_1' a_0'\underline{A}^2\underline{B}^3\underline{C}^3\underline{DE}f(t-.412)$
24	$2b_1\underline{b}_1^2\underline{b}_2^2\underline{a}_3\underline{b}_2'^2 a_0'^2\underline{b}_2 a_4\underline{b}_3'\underline{b}_1'^2\underline{A}^3\underline{B}^4\underline{C}^3\underline{DE}f(t-.444)$
25	$2\underline{b}_1^3\underline{b}_2\underline{a}_2' b_1'\underline{b}_1'^2\underline{b}_2 a_4\underline{b}_3'\underline{b}_2' a_0'^2\underline{a}_2\underline{A}^3\underline{B}^4\underline{C}^2\underline{DE}f(t-.448)$
26a	$2b_1\underline{b}_1^3\underline{b}_2\underline{a}_2'\underline{b}_1'^3 a_0'^3\underline{b}_2 a_4\underline{b}_2'\underline{b}_2'\underline{a}_2\underline{A}^4\underline{B}^4\underline{C}^2\underline{DE}f(t-.480)$
26b	$b_1\underline{b}_1^3\underline{b}_2^4\underline{a}_2^2\underline{b}_2'^4\underline{b}_1'^4 a_0'^3\underline{a}_3^2\underline{A}^4\underline{B}^8\underline{C}^4\underline{E}f(t-.480)$
27	$\underline{b}_1^2\underline{b}_2^3\underline{a}_2^2\underline{b}_2'^3\underline{a}_1' b_1'\underline{b}_1' a_0'\underline{b}_3 a_4\underline{b}_2'\underline{A}^2\underline{B}^5\underline{C}^4\underline{DE}f(t-.512)$
28	$3\underline{b}_1^3\underline{b}_2^3\underline{a}_2^2\underline{b}_2'^3 b_1'\underline{b}_1'^2 a_0'^2\underline{b}_2 a_4\underline{b}_2'\underline{A}^3\underline{B}^6\underline{C}^4\underline{DE}f(t-.540)$
29	$3b_1\underline{b}_1^3\underline{b}_2^3\underline{a}_2^2\underline{b}_2'^3\underline{b}_1'^3 a_0'^3\underline{b}_2 a_4\underline{b}_3'\underline{A}^4\underline{B}^6\underline{C}^4\underline{DE}f(t-.572)$
30a	$\underline{b}_1^2\underline{a}_2 b_1'\underline{b}_1'(a_4\underline{b}_2\underline{b}_3')^2\underline{b}_2\underline{b}_2' a_0'\underline{a}_2'\underline{A}^2\underline{B}^3\underline{C}^3\underline{D}^2\underline{E}f(t-.600)$
30b	$(\underline{b}_1\underline{b}_2)^2(a_4\underline{b}_2\underline{b}_3')^2\underline{b}_1' b_1'\underline{b}_2'^2 a_0'\underline{A}^2\underline{B}^4\underline{C}^4\underline{D}^2\underline{E}f(t-.600)$

Table 3. The wave trains which arrive at P_1 between 0 and 0.6 microsecond, the upper and middle crossarms being omitted.

1	$1(t)$	9	$(\underline{a}_3 a'_0)^3 1(t-.384)$
2	$\underline{a}_3 1(t-.096)$	10	$2\underline{b}_3 a_4 \underline{b}'_3 \underline{a}_3 a'_0 \underline{D} 1(t-.412)$
3	$a_3 a'_0 1(t-.128)$	11	$2\underline{b}_2 a_4 \underline{b}'_3 \underline{a}_3 a'^2_0 \underline{D} 1(t-.444)$
4	$\underline{a}^2_3 a'_0 1(t-.224)$	12	$\underline{a}^4_3 a'^3_0 1(t-.480)$
5	$(a_3 a'_0)^2 1(t-.256)$	13	$(\underline{a}_3 a'_0)^4 1(t-.512)$
6	$\underline{b}_3 a_4 \underline{b}'_3 \underline{D} 1(t-.284)$	14	$3\underline{b}_2 a_4 \underline{b}'_3 \underline{a}^2_3 a'^2_0 \underline{D} 1(t-.540)$
7	$\underline{b}_3 a_4 \underline{b}'_3 a' \underline{D} 1(t-.316)$	15	$3\underline{b}_3 a_4 \underline{b}'_3 \underline{a}^2_2 a'^3_0 \underline{D} 1(t-.572)$
8	$\underline{a}^3_3 a'^2_0 1(t-.352)$	16	$(\underline{b}_3 a_4 \underline{b}'_3 \underline{D})^2 a'_0 1(t-.600)$

Table 4. Table 3 with numerical values.

1	$1(t)$	$=1(t)$
2	$-.52\underline{\alpha}_3 1(t-.096)$	$=[-.52\phi(-.096)+.374\phi(-.132)-.082\phi(-.168)+.018\phi(-.204)]1(t)$
6	$-.288\underline{\beta}^2_3 \underline{D} 1(t-.284)$	$=[-.288\phi(-.284)-.45\phi(-.320)-.077\phi(-.356)+.055\phi(-.392)-.026\phi(-.428)-.06\phi(-.472)+.042\phi(-.508)+.162\phi(-.544)+.011\phi(-.580)-.032\phi(-.616)] \times 1(t)$

Table 5. Table 3 with numerical values different from Table 4.

1	$1(t)$	$=1(t)$
2	$-.45\underline{\alpha}_3 1(t-.096)$	$=[-.45\phi(-.096)+.49\phi(-.132)-.054\phi(-.168)]1(t)$
6	$-.245\underline{\beta}^2_3 \underline{D} 1(t-.284)$	$=[-.245\phi(-.284)-.436\phi(-.320)-.146\phi(-.356)+.037\phi(-.392)-.089\phi(-.472)-.061\phi(-.508)+.109\phi(-.544)+.053\phi(-.580)]1(t).$

Table 6. Based on Table 3, the crossarms being represented by a capacitance.

1	$1(t)$	$=1(t)$
2	$\underline{a}_3 1(t-.096)$	$=[-.791\varepsilon^{-86(t-.096)}-.209]1(t-.096)$
6a	$\underline{b}_3 a_4 \underline{b}_3' 1(t-.284)$	$=[-.775+.775\varepsilon^{-86(t-.284)}+67.5(t-.284)\varepsilon^{-86(t-.284)}]1(t-.284).$
6b	$\underline{b}_3 a_4^2 \underline{b}_3' \underline{a}_3' 1(t-.472)$	$=[+.131-.131\varepsilon^{-86(t-.472)}-11.3(t-.472)\varepsilon^{-86(t-.472)}-34\times 82(t-.472)^2\times \varepsilon^{-86(t-.472)}]1(t-.472).$

Table 7. The wave trains which arrive and are refracted at the tip of the upper crossarms between 0 and 0.6 microsecond. The middle and bottom crossarms are omitted.

1	$b_1\underline{E}1(t)$	$=[1.1-.121\phi(-.036)+.013\phi(-.072)]1(t)$
2	$\underline{b}_1 a_4 b_1' \underline{E}1(t-.284)$	$=[-.49\phi(-.284)-.382\phi(-.320)+.09\phi(-.356)-.016\phi(-.392)]1(t)$
3	$\underline{b}_1 a_4^2 \underline{a}_3' b_1' \underline{E}1(t-.568)$	$=[-.146\phi(-.568)+.045\phi(-.604)]1(t).$

Table 8. Table 7 using Heaviside's operators and $b_1\underline{E}$ made equal to unity.

1	$=1(t)$
2	$=-.81[1-\varepsilon^{-68(t-.284)}]1(t-.284)$
3	$=-.655\times 68(t-.568)\varepsilon^{-68(t-.568)}\times 1(t-.568)$

Table 9. The wave trains that arrive at P_1 between 0 and 0.6 microsecond. The crossarms are integral parts of the tower top.

1	$1(t)$	6	$-.322\underline{D}1(t-.316)$
2	$0.23\times 1(t-.096)$	7	$-.148\underline{D}1(t-.412)$
3	$0.097\times 1(t-.128)$	8	$-.062\underline{D}1(t-.444)$
4	$0.022\times 1(t-.224)$	9	$-.021\underline{D}1(t-.540)$
5	$-.768\underline{D}1(t-.284)$	10	$0.247\underline{D}1(t-.600)$

$$\underline{D} = 1-0.186\Phi(-.188)$$

Table 10. Table 2 with numerical values and $f(t)=1(t)$.

1	$0.55\underline{E}1(t)$
2	$-.136\underline{\alpha}_2\underline{\beta}'_1\underline{BE}1(t-.050)$
4	$-.048\underline{\beta}_1\underline{\beta}_2\underline{\alpha}_2\underline{\beta}'_2\underline{B}^2\underline{CE}1(t-.096)$
9	$-.003\underline{\beta}_1\underline{\beta}_2^2\underline{\alpha}_2^2\underline{\beta}'^2_2\underline{\alpha}'_1\underline{B}^3\underline{C}^2\underline{E}1(t-.192)$
14	$-.026\underline{\beta}_1\underline{\beta}_2\underline{\beta}_3\underline{\beta}'_2\underline{\beta}'_2\underline{B}^2\underline{C}^2\underline{DE}1(t-.284)$
20	$-.002\underline{\beta}_2\underline{\beta}_2^2\underline{\alpha}_2\underline{\beta}'^2_2\underline{\beta}_3\underline{\beta}'_3\underline{\alpha}'_1\underline{B}^3\underline{C}^3\underline{DE}1(t-.380)$

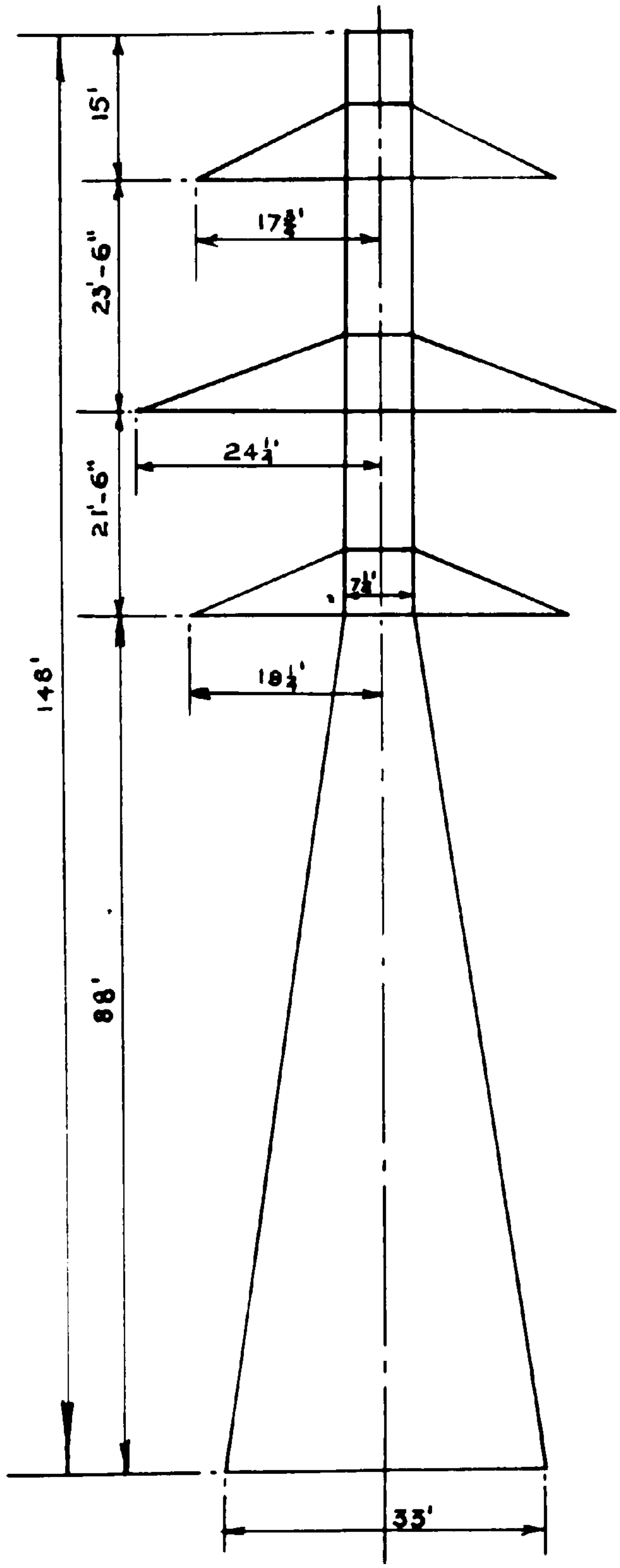

Fig.1. A typical 345-kv Double Circuit Suspension Tower.

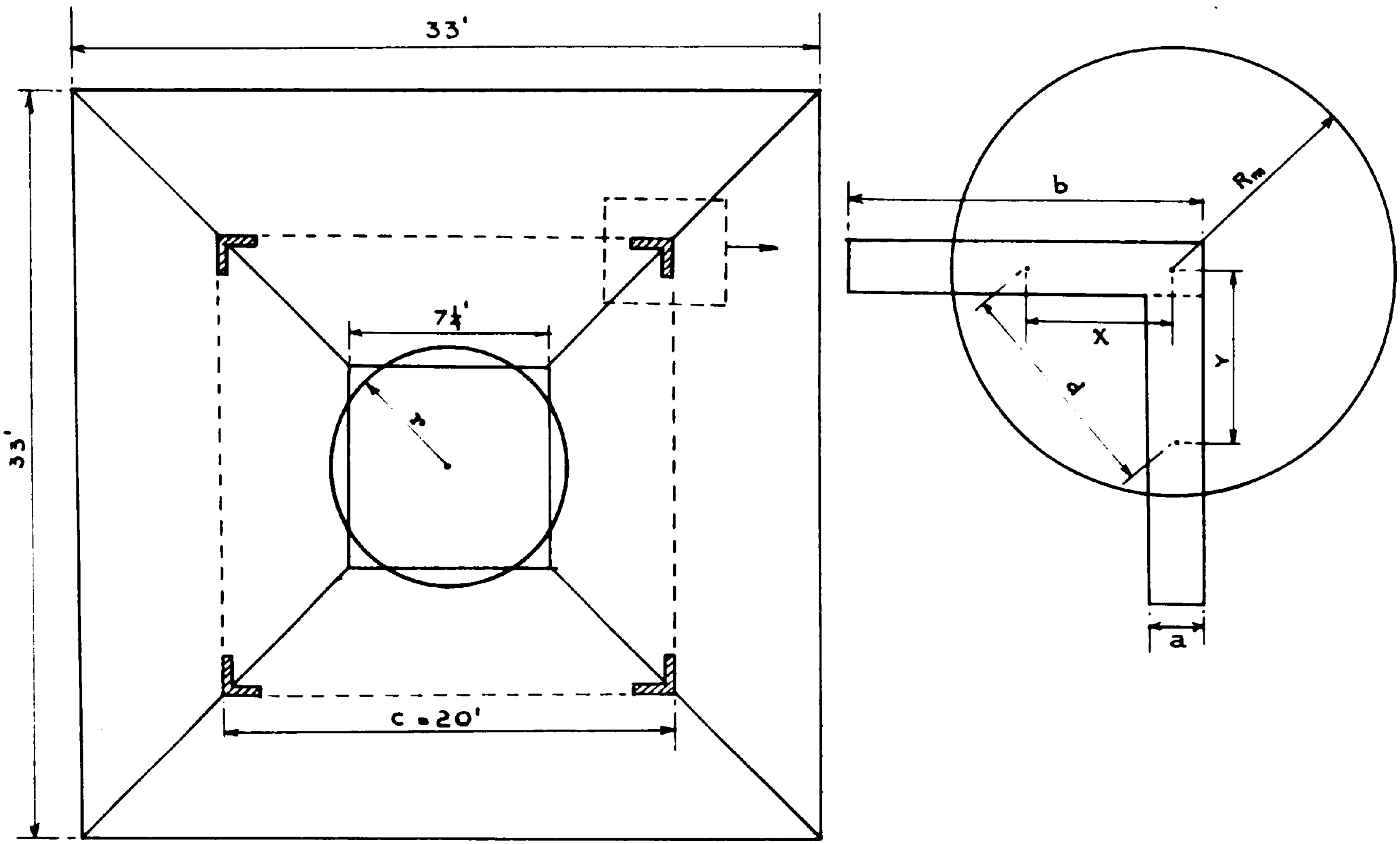

Fig.2. Tower leg with equivalent cylinder.

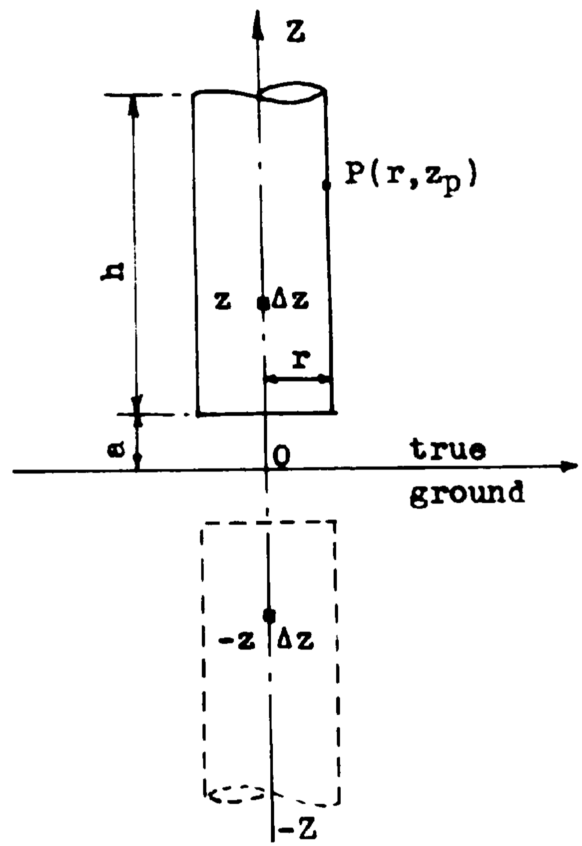

Fig.3. Equivalent cylinder and image.

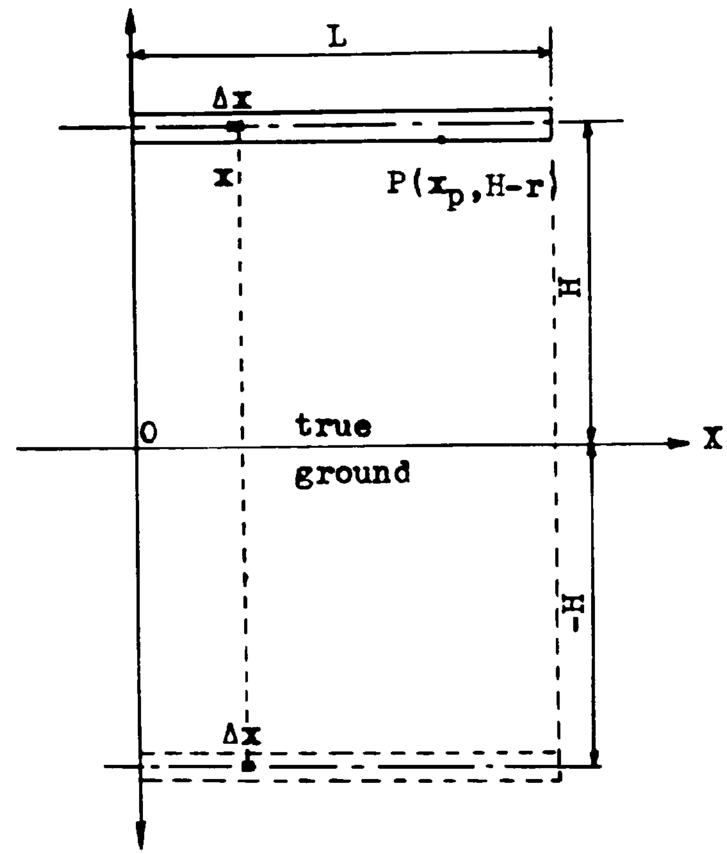

Fig.4. Crossarm and image.

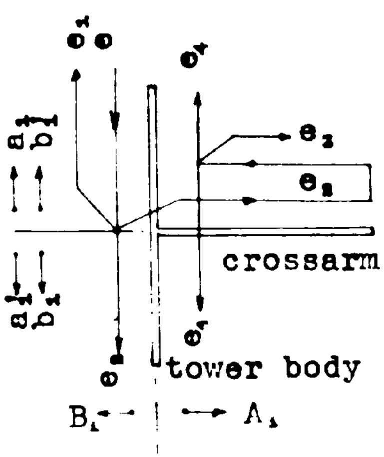

Fig.5. Reflected and transmitted waves on tower body with cross-arm.

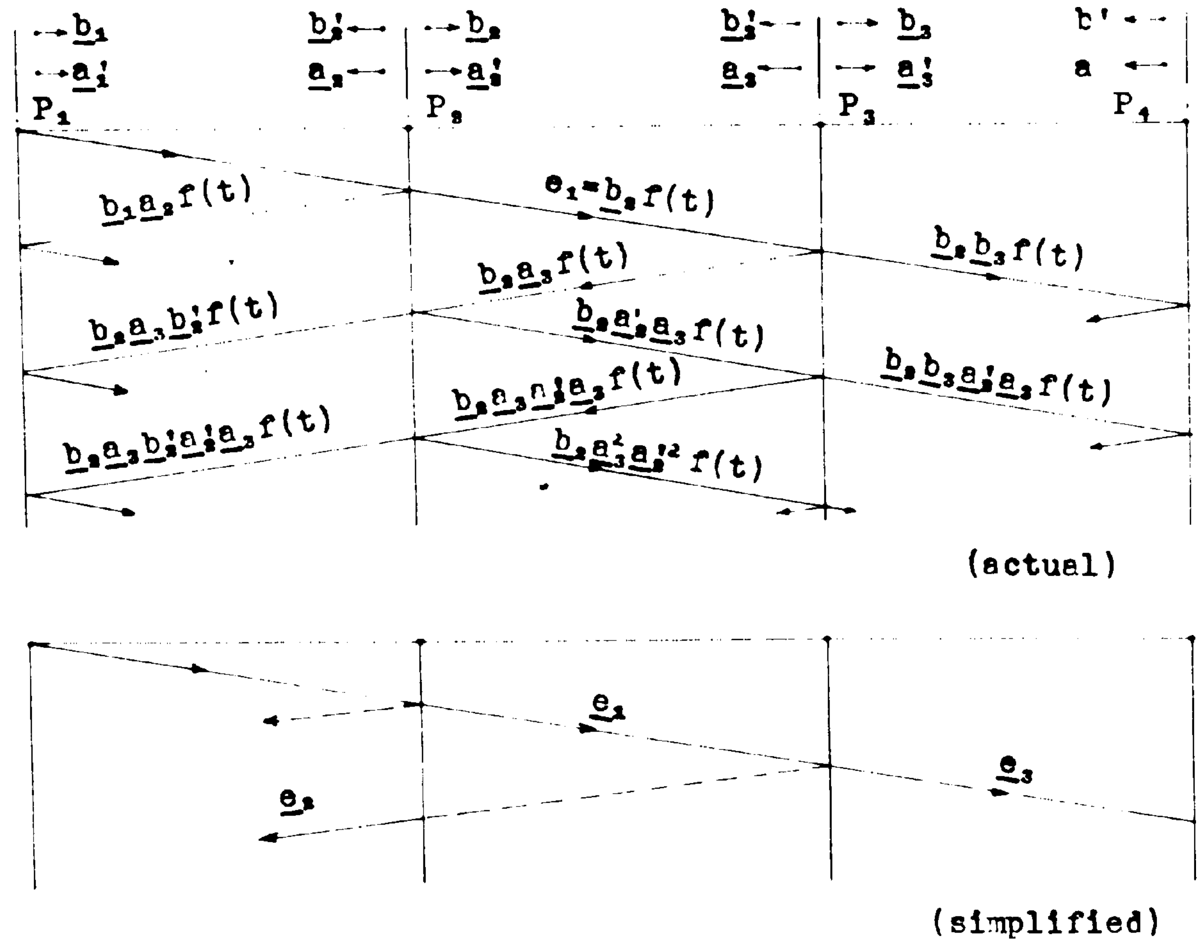

Fig.6. Sample lattice diagram using wave trains and operators.

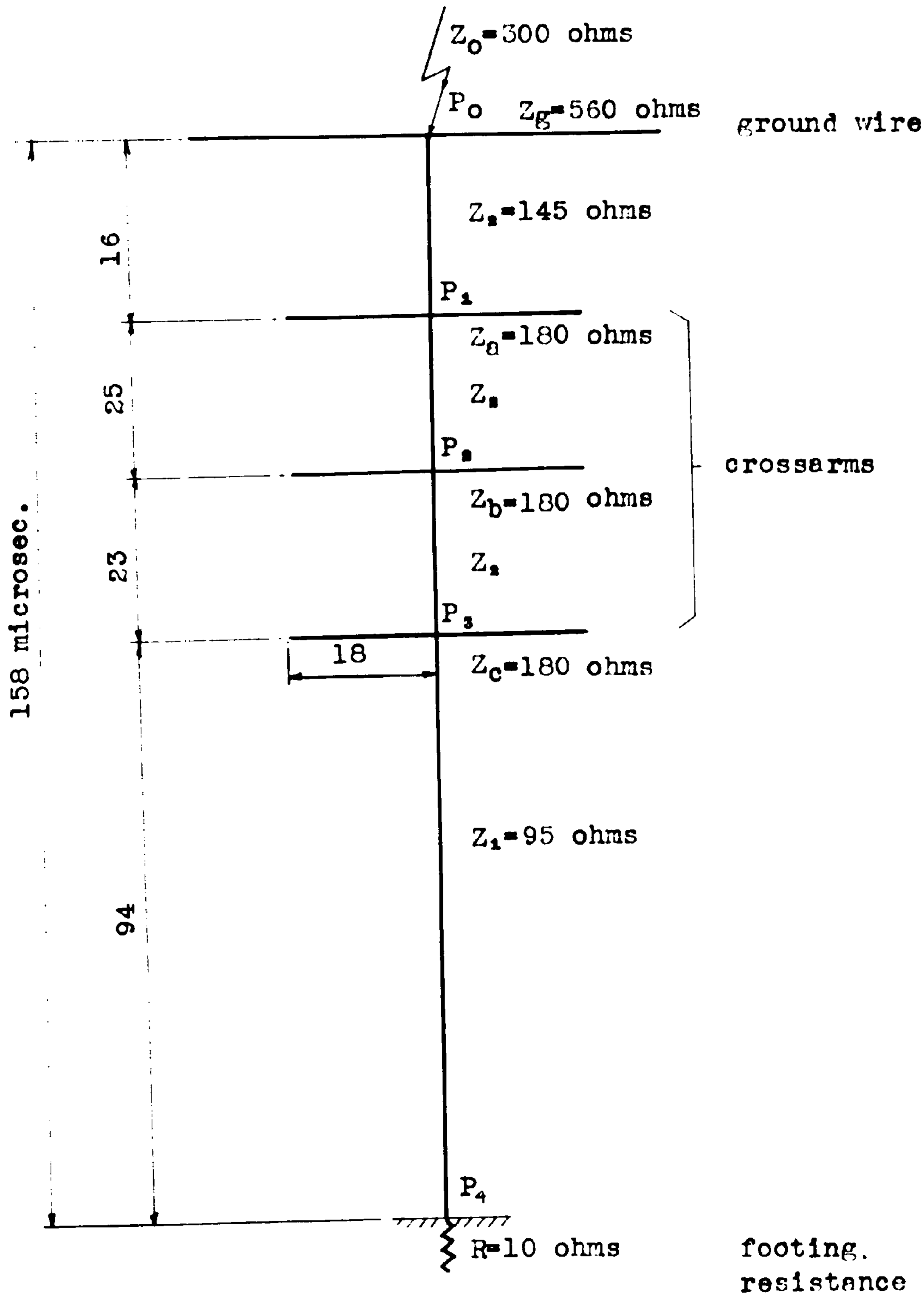

Fig. 7. A 345-kv tower represented by surge impedances of parts.

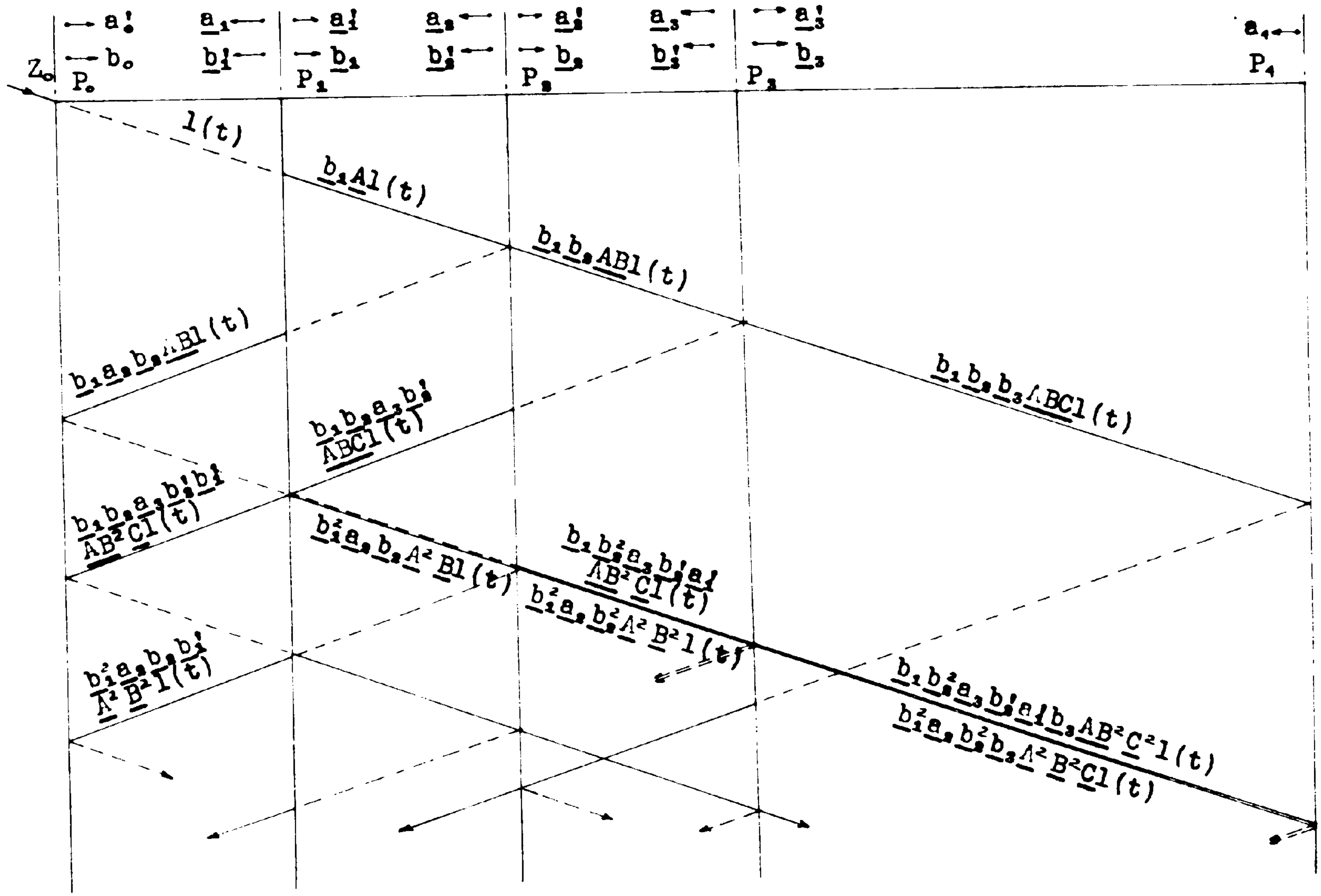

Fig.8. Plan of complete lattice diagram for a 345-kv transmission line tower. (not to scale)

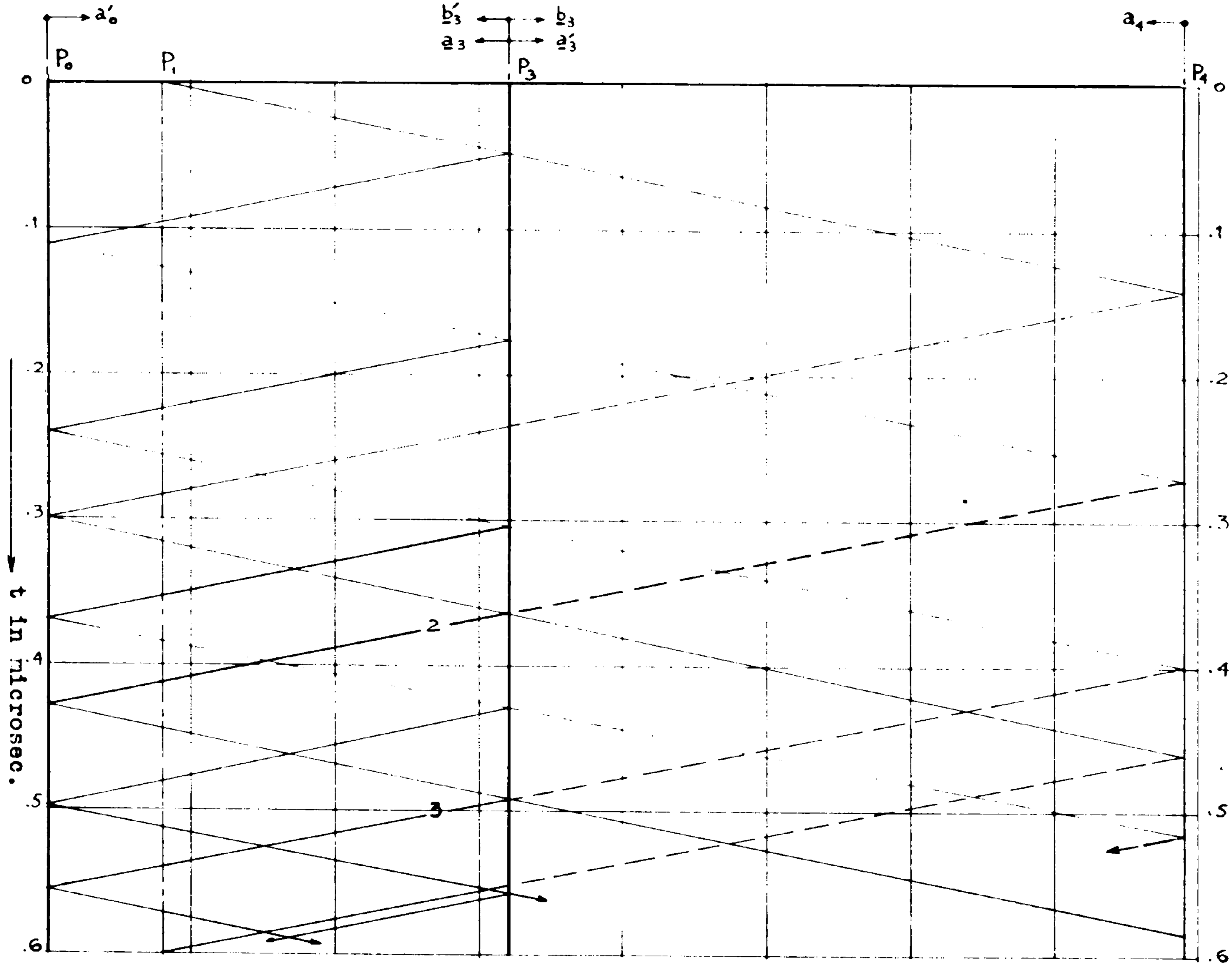

Fig. 9. Complete lattice diagram for a 345-kv tower with bottom crossarms only.

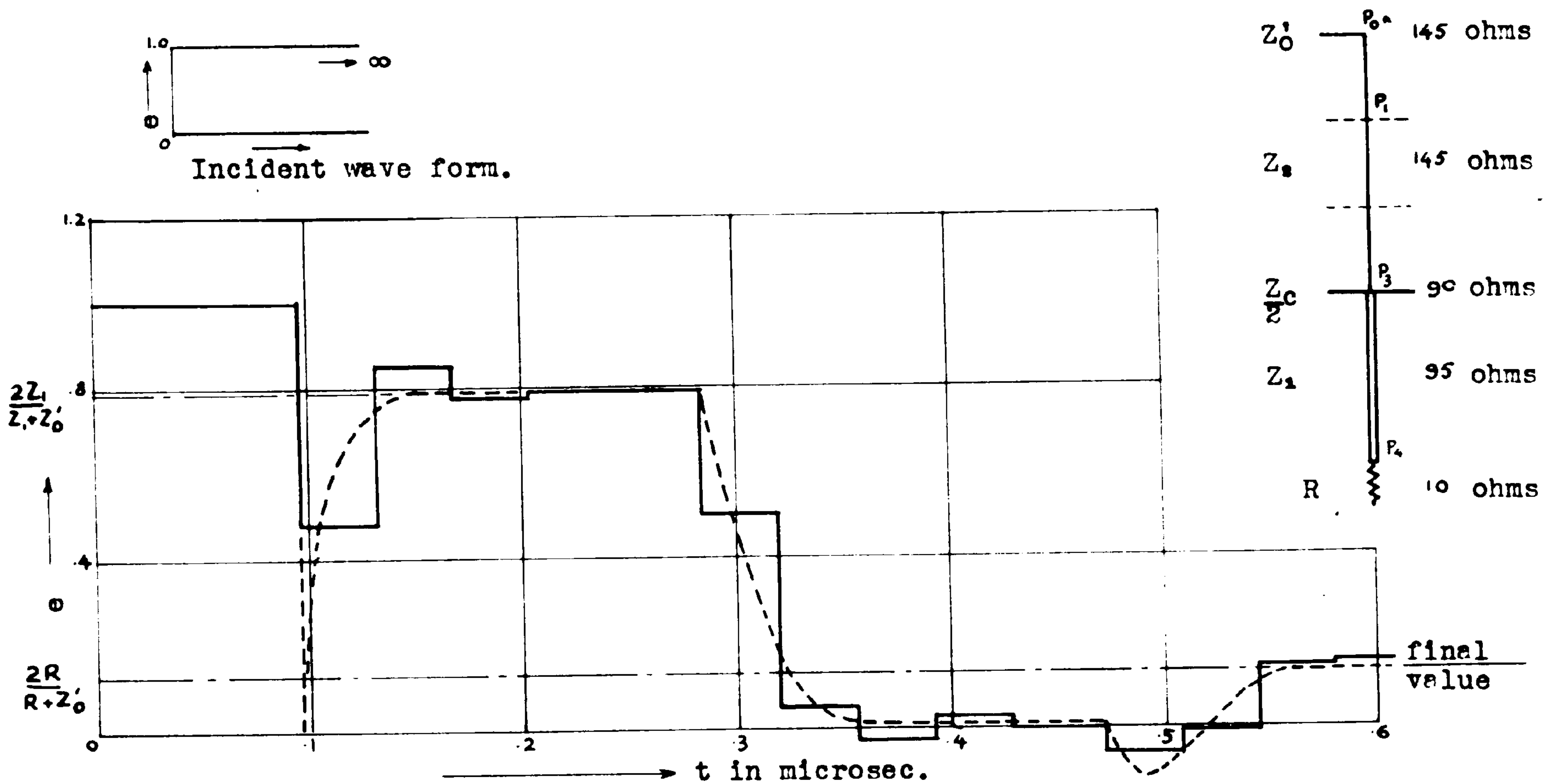

Fig.10. Surge voltage at P_1 due to an abrupt unit wave. Tower has only bottom crossarms.
(Solid lines): Crossarm represented by a surge impedance.
(Broken lines): Crossarm represented by a lumped capacitance.

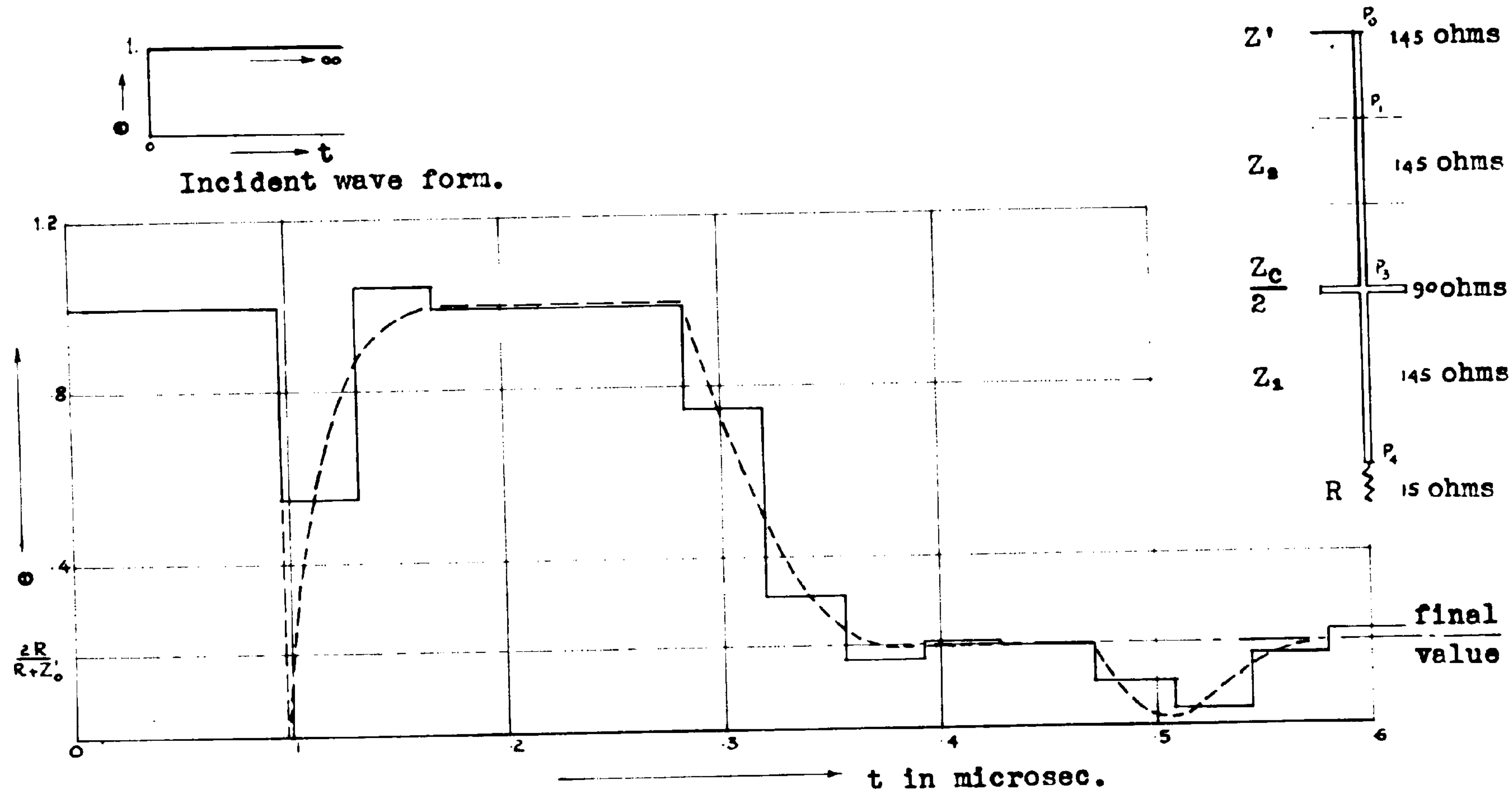

Fig. 11. Surge voltage at P_1 due to an abrupt unit wave. Tower has only bottom crossarms. (Solid lines): Crossarm represented by a surge impedance. (Broken lines): Crossarm represented by a lumped capacitance.

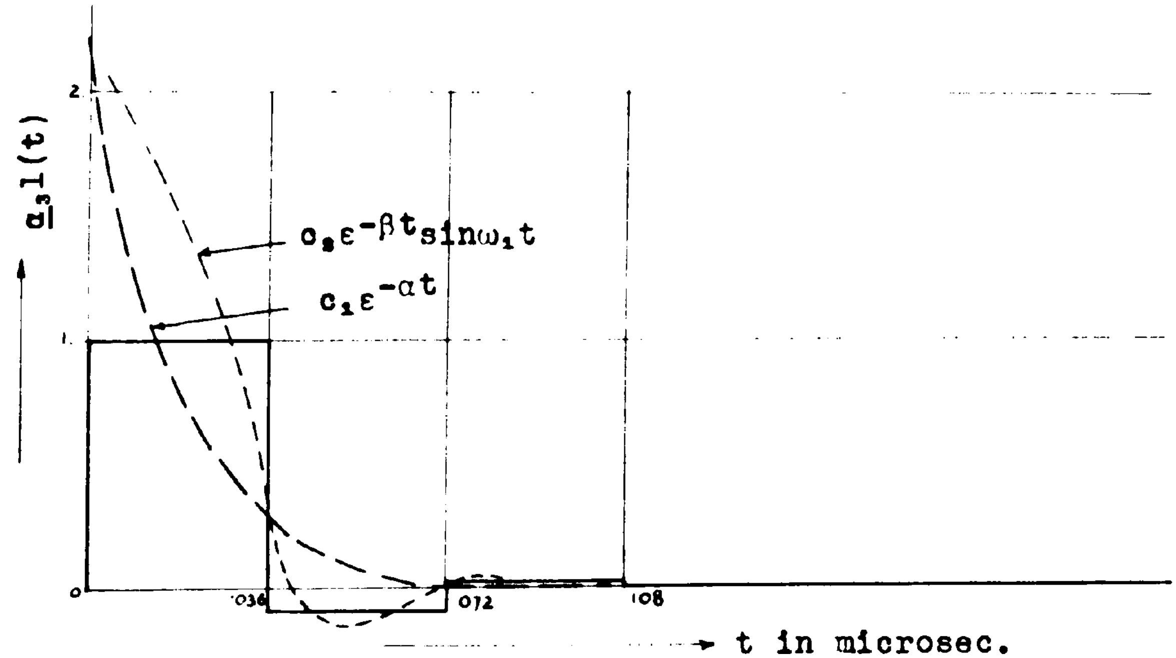

Fig.12. $\underline{a}_3 1(t)$ resolved into components.

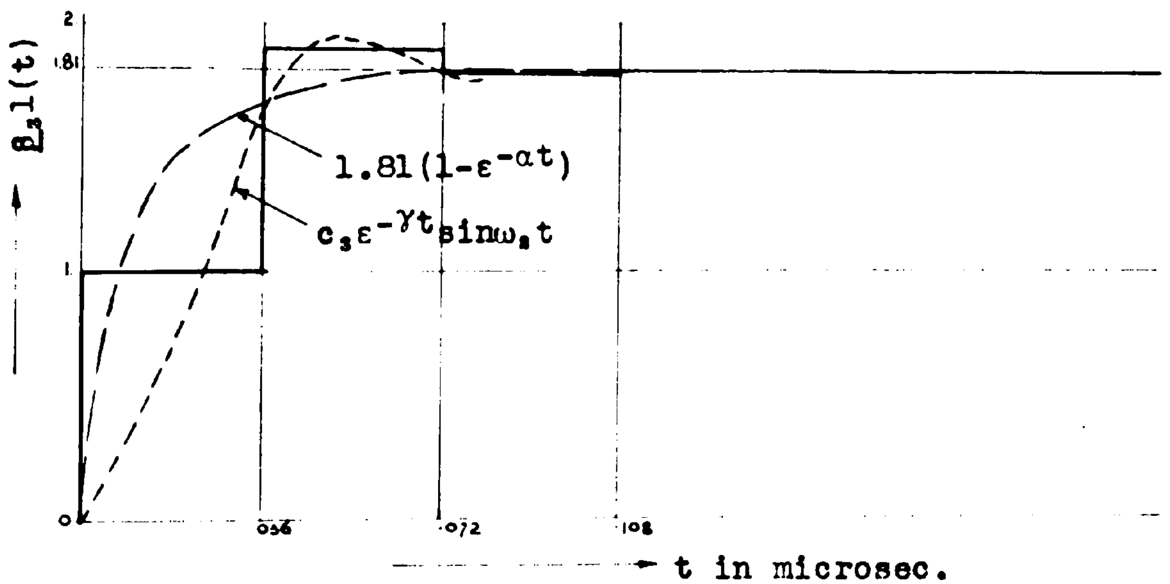

Fig.13. $\underline{\beta}_3 1(t)$ resolved into components.

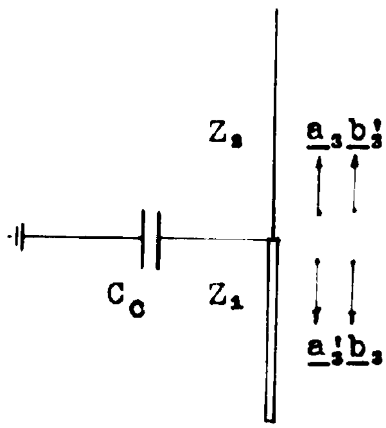

Fig. 14. Crossarms represented by
an equivalent capacitance.

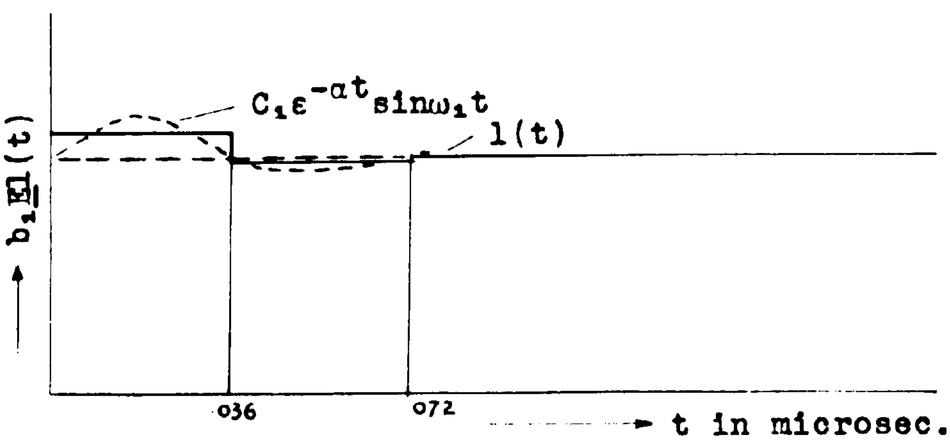

Fig. 17. $b_1\underline{\Xi}1(t)$ resolved into components.

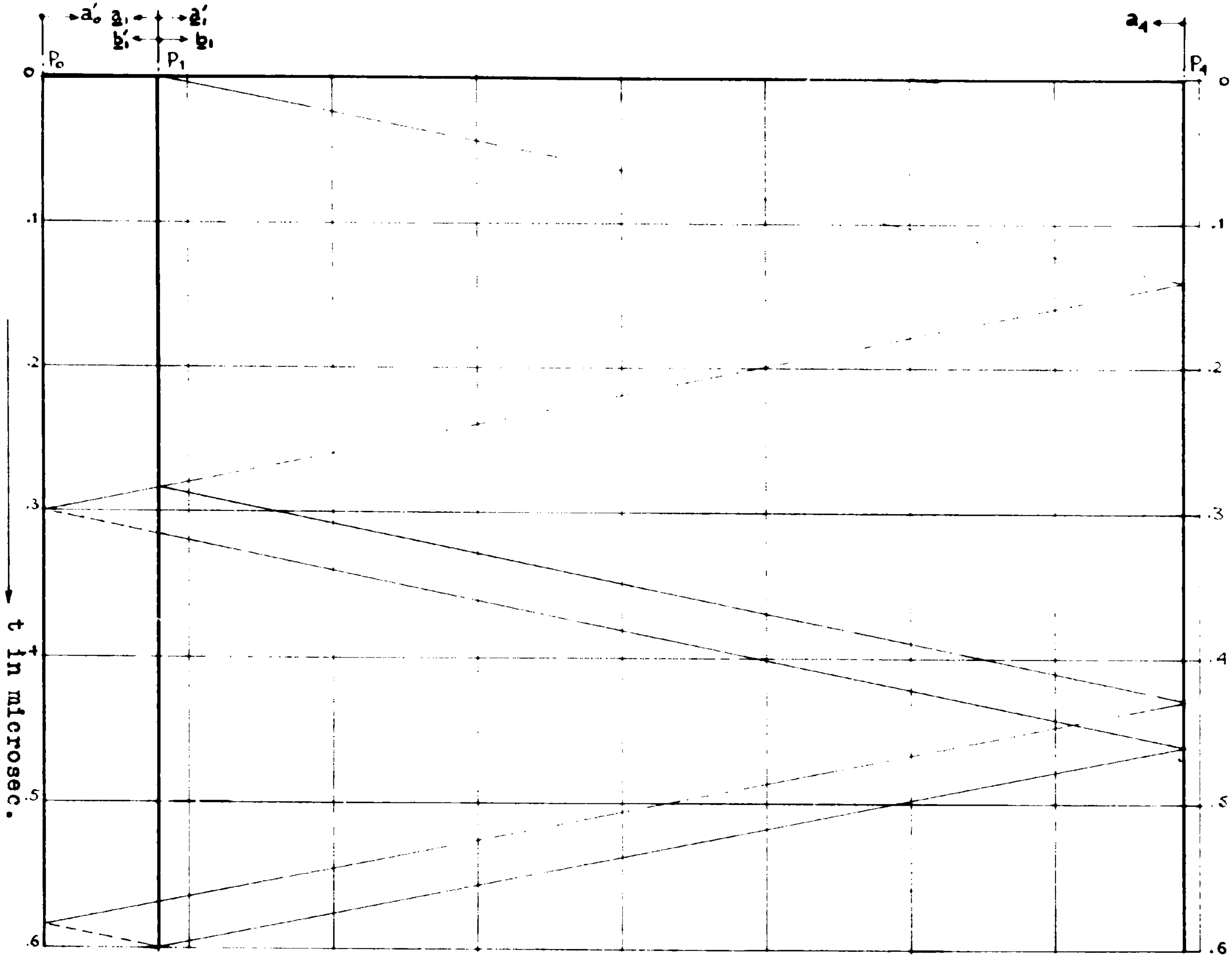

Fig.15. Complete lattice diagram for a 345-kv tower with upper crossarms only and $Z_1 = Z_2$

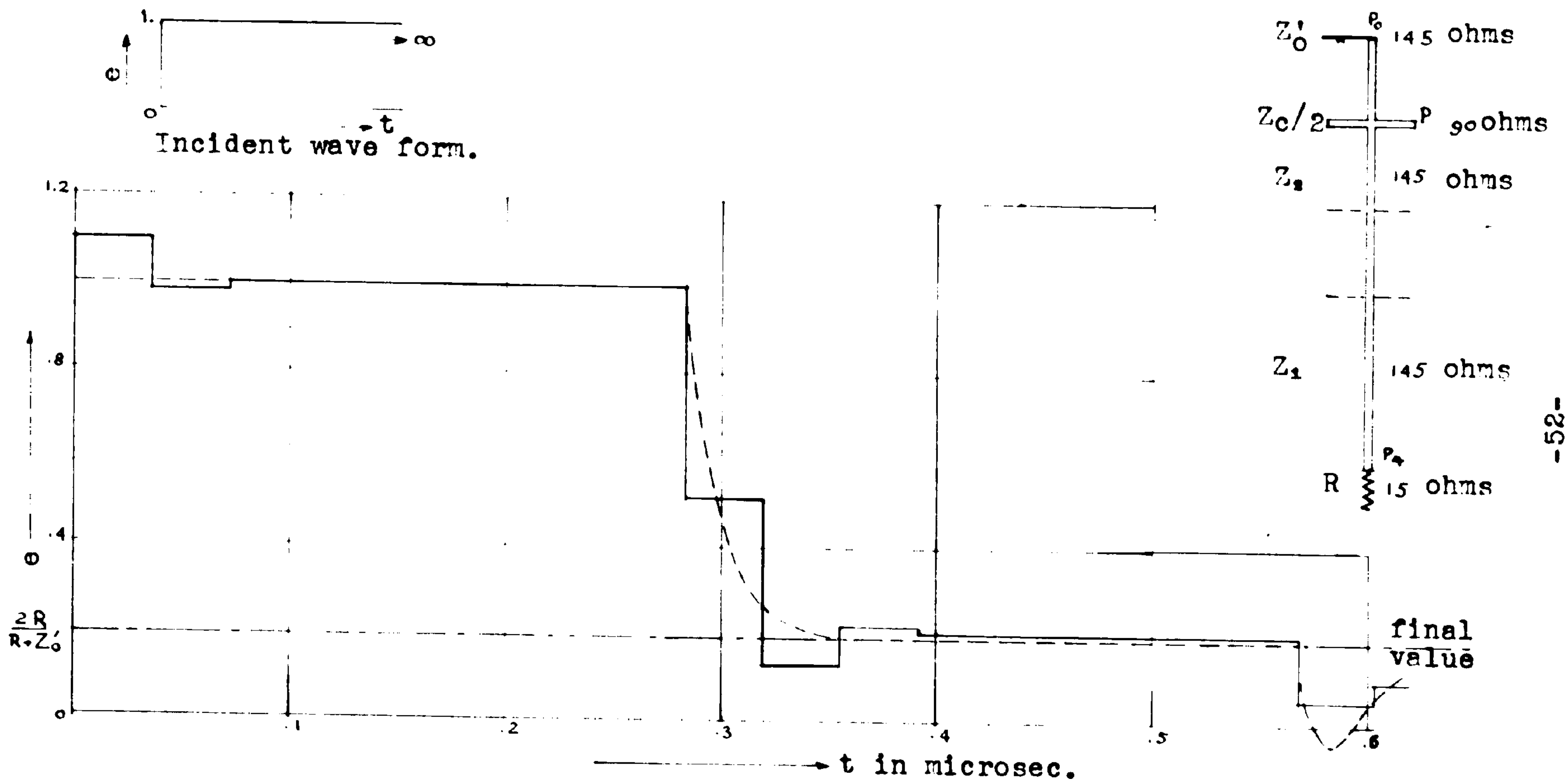

Fig.16. Surge voltage at P (tip of the upper crossarms) due to an abrupt unit wave.
Tower has upper crossarms only.
(Solid lines) : Crossarm represented by surge impedance.
(Broken lines): Crossarm represented by lumped capacitance.

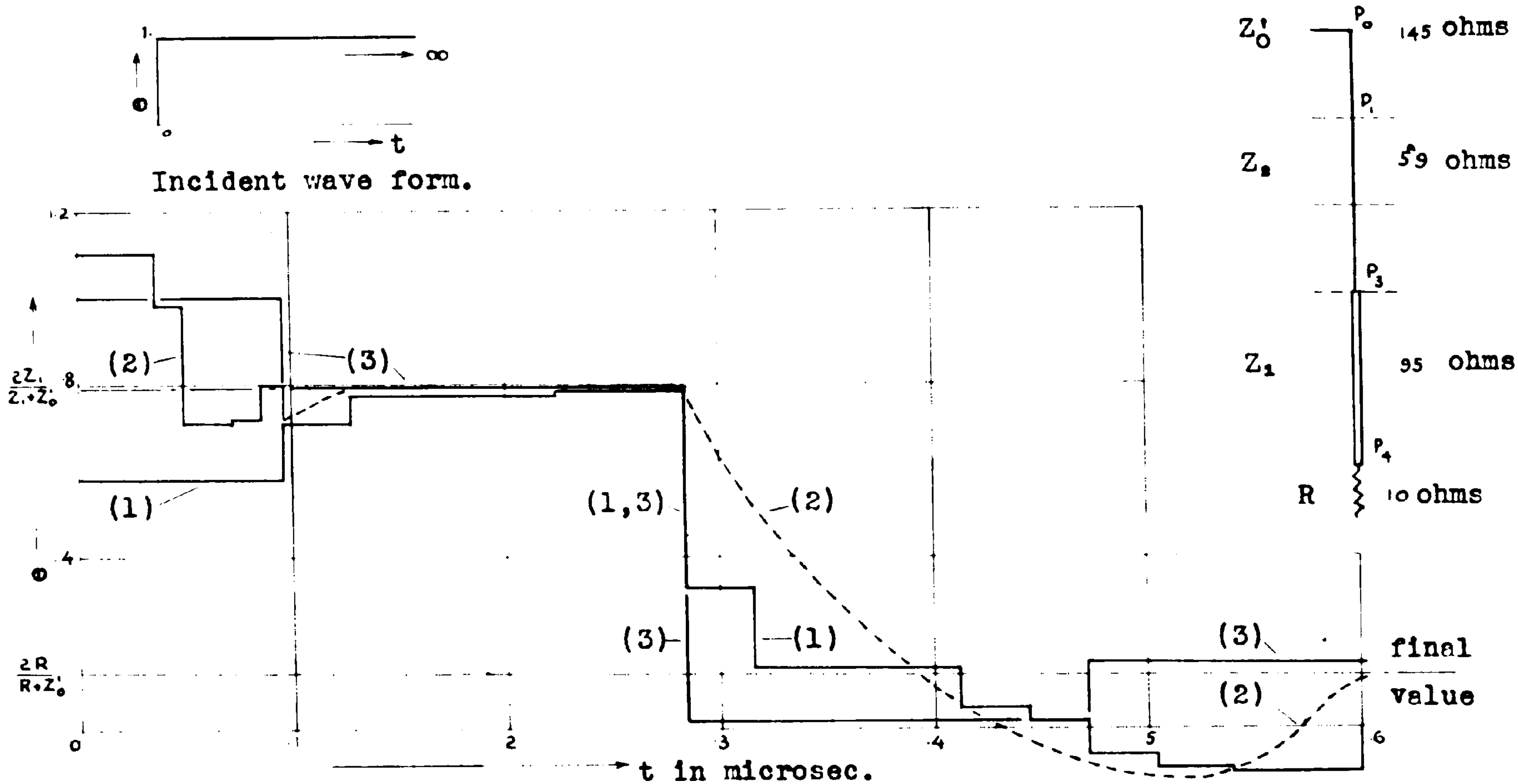

Fig. 18. Surge voltage at P_1 due to an abrupt unit wave.
(1): Crossarms form an integral part of tower top.
(2): Crossarms represented by surge impedances. Broken lines indicate the axis of oscillations.
(3): Crossarms omitted.

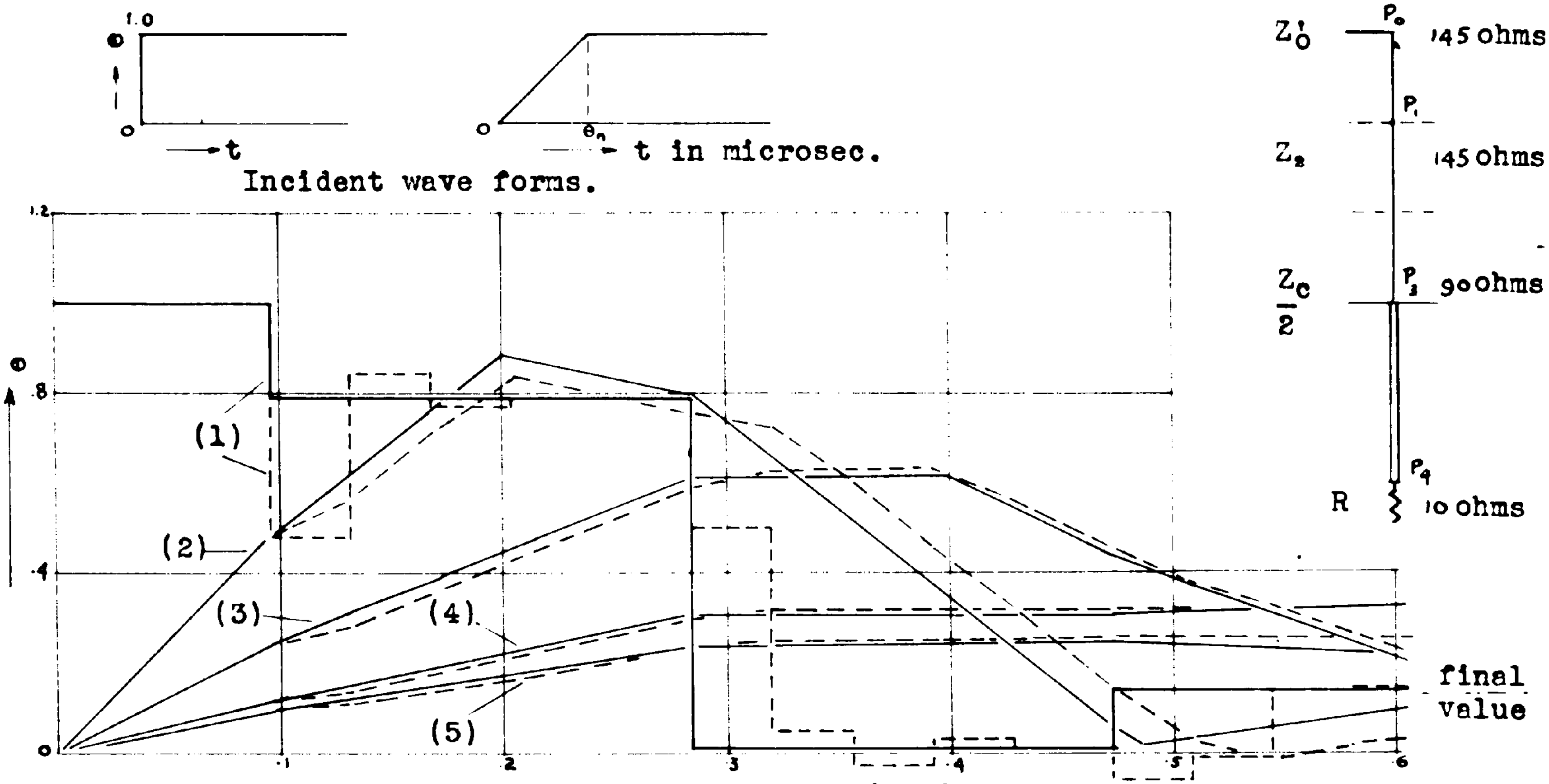

Fig. 19. Surge voltage at P_1.
(1): Due to an abrupt unit wave.
(2): Due to a unit wave with 0.2 μs front.
(3): With 0.4 μs front. (solid lines): Tower has no crossarms.
(4): With 0.8 μs front. (broken lines): Tower has crossarms at P_3.
(5): With 1.0 μs front.

BIBLIOGRAPHY

1. Two-Year Lightning Experience on 345-Kv Lines, H. L. Rorden, E. S. Zobel, G. D. Lippert. AIEE Transactions No. 33, Dec. 1957, pp. 954-58.

2. 1956 Lightning Field Investigation on the OVEC 345-Kv System, R. H. Schlomann, W. S. Price, I. B. Johnson, J. G. Anderson. AIEE Transactions No. 34, Febr. 1958, pp. 1447-56.

3. Field Studies of the Surge Response of a 345-Kv Transmission Tower and Ground Wire, G. D. Breuer, A. J. Schultz, R. H. Schlomann, W. S. Price. AIEE Transactions No. 34, Febr. 1958, pp. 1392-96.

4. Lightning Performance of 138-Kv Twin-Circuit Transmission Lines of Commonwealth Edison Company - Operating Experience and Field Studies, R. W. Caswell, I. B. Johnson, E. F. Koncel, Jr., N. R. Schultz. AIEE Transactions No. 34, Febr. 1958, pp. 1480-89.

5. La Foudre et ses Effets sur les Lignes Aeriennes, C. L. Fortesque, (Report). Congres International d'Electricite, Paris, 1932.

6. Electromagnetic Waves and Radiating Systems (Book), Edward C. Jordan. Prentice-Hall, Inc., New York.

7. Lightning Computations for Transmission Lines with Overhead Ground Wires (Part II), C. A. Jordan. General Electric Review, Vol. 37 No. 4, April 1934.

8. Traveling Waves on Transmission Systems (Book), L. V. Bewley. John Wiley & Sons, Inc. New York. Chapman & Hall, Ltd. London, 1951.

9. Heaviside's Operational Calculus as Applied to Engineering and Physics (Book), E. J. Berg. McGraw-Hill Book Company, 1936.

VITA

The author was born as the elder son of Rev. Domitian and Theresianna Tambunan on May 29, 1921 in Lumbanlobu, Tapanuli, Sumatra, Indonesia.

He graduated in 1951 from the College of Engineering and Technology of the National Council of Education, Bengal, India, with a Bachelor of Electrical Engineering degree. In June, 1952, he received the Master of Science degree in Electrical Engineering from Lehigh University.

Following graduation he was employed by the Government of the Republic of Indonesia as Ass. Manager of the Division of Electric Power Generation and Transmission, Ministry of Public Works and Energy, Djakarta, Indonesia. In October, 1954 and March, 1956 he represented his government in the "ECAFE" (Economic Commission For Asia and the Far East) conference on electric power.

Since September, 1956, he has held the position of instructor in the department of Electrical Engineering at Lehigh University.